



HAL
open science

INVARIANT DOMAIN PRESERVING APPROXIMATIONS FOR THE EULER EQUATIONS WITH TABULATED EQUATION OF STATE

Bennett Clayton, Jean-Luc Guermond, Bojan Popov

► **To cite this version:**

Bennett Clayton, Jean-Luc Guermond, Bojan Popov. INVARIANT DOMAIN PRESERVING APPROXIMATIONS FOR THE EULER EQUATIONS WITH TABULATED EQUATION OF STATE. 2021. hal-03224638

HAL Id: hal-03224638

<https://hal.science/hal-03224638v1>

Preprint submitted on 11 May 2021

HAL is a multi-disciplinary open access archive for the deposit and dissemination of scientific research documents, whether they are published or not. The documents may come from teaching and research institutions in France or abroad, or from public or private research centers.

L'archive ouverte pluridisciplinaire **HAL**, est destinée au dépôt et à la diffusion de documents scientifiques de niveau recherche, publiés ou non, émanant des établissements d'enseignement et de recherche français ou étrangers, des laboratoires publics ou privés.

1 **INVARIANT DOMAIN PRESERVING APPROXIMATIONS FOR THE EULER**
2 **EQUATIONS WITH TABULATED EQUATION OF STATE ***

3 BENNETT CLAYTON[†], JEAN-LUC GUERMOND[†], AND BOJAN POPOV[†]

4 **Abstract.** This paper is concerned with the approximation of the compressible Euler equations supplemented
5 with an equation of state that is either tabulated or is given by an expression that is so involved that solving
6 elementary Riemann problems is hopeless. A robust first-order approximation technique that guarantees that the
7 density and the internal energy are positive is proposed. A key ingredient of the method is a local approximation of
8 the equation of state using a co-volume ansatz from which upper bounds on the maximum wave speed are derived
9 for every elementary Riemann problem.

10 **Key words.** Compressible Euler equations, tabulated equation of state, maximum wave speed, Riemann prob-
11 lem, Invariant domain preserving approximation, composite waves

12 **AMS subject classifications.** 65M60, 65M12, 65M22, 35L65

13 **1. Introduction.** In many important applications, the compressible Euler equations are sup-
14 plemented with an equation of state that is either tabulated or given by a complicated analytic
15 expression. Throughout the paper, we will refer to this type of equation of state as the ‘oracle’. In
16 this case, approximating the Euler equations while guaranteeing positivity of the density and posi-
17 tivity of the internal energy is problematic since no exact solution of elementary Riemann problems
18 can be a priori inferred. Solving a Riemann problem when the equation of state is analytically
19 well defined is feasible, though possibly expensive, (see e.g., Colella and Glaz [5, §1], Ivings et al.
20 [16], Quartapelle et al. [24]). This cannot be efficiently done with an oracle for this requires inter-
21 polating/approximating the equation of state, and to the best of our knowledge, there is no clear
22 technique to do so in the literature. Various methods to avoid this problem have been proposed in
23 the literature. For instance, one can use approximate Riemann solvers like in Dukowicz [7], [5, §2],
24 Roe and Pike [26], Pike [23], or simplify the Riemann problem by using flux splitting techniques
25 like in Toro et al. [28]. However, for most of these techniques very little is guaranteed besides
26 positivity of the density, which is not difficult to achieve. The objective of the paper is to address
27 these questions. More precisely, we propose an approximation method to solve the Euler equations
28 equipped with an oracle. This is done by adapting the technique from Guermond and Popov [12]
29 where invariant-domain properties are obtained by ascertaining that they hold true for elementary
30 Riemann problems. The key is to augment each elementary Riemann system with an additional
31 scalar equation and replace the oracle by a covolume equation of state where the coefficient γ is
32 variable and obtained as the solution to the additional equation. This idea is adapted from Abgrall
33 and Karni [1]. A variation of this idea is also employed in [5, Eq. (37)] and Pantano et al. [22,
34 Eq. (22)]. The proposed algorithm is explicit in time and preserves the positivity of the density and
35 the internal energy under an appropriate CFL restriction on the time step. Additional properties
36 can be preserved depending on the nature of the oracle. As in Guermond et al. [14], the method is
37 agnostic to the space approximation. An interesting feature of the method is that it automatically
38 recovers the standard co-volume behaviour if the oracle is indeed a covolume equation of state. In

*This material is based upon work supported in part by the National Science Foundation grant DMS-1619892, by the Air Force Office of Scientific Research, USAF, under grant/contract number FA9550-18-1-0397, the Army Research Office, under grant number W911NF-15-1-0517, and the U.S. Department of Energy by Lawrence Livermore National Laboratory under Contracts B640889.

[†]Department of Mathematics, Texas A&M University 3368 TAMU, College Station, TX 77843, USA.

39 compliance with Godunov’s theorem, the method is first-order accurate in space, however, achieving
 40 higher-order accuracy in space is out of the scope of this paper. This can be done by implementing
 41 the convex limiting technique described in [13, 14]. This work is in progress and will be reported
 42 elsewhere.

43 The paper is organised as follows. The problem and the notation are introduced in §2. The
 44 space and time approximation method from [12] is also briefly recalled in this section. The main
 45 motivation of the paper is given at the end of §2.2. We introduce an extended Riemann problem
 46 in §3. The key point of this section is summarized in Remark 3.1. An exact weak solution to the
 47 extended Riemann problem is constructed in §4. It is also shown in this section that this weak
 48 solution satisfies the expected invariant domain-properties. The main results of §4 are Lemma 4.4,
 49 Lemma 4.5 and Theorem 4.6. An upper bound on the maximum wave speed for the extended
 50 Riemann problem is derived in §5. This upper bound is the key piece of information that is needed
 51 for practitioners who may have little interest in the Riemann problem theory (see §5.2–§5.5). The
 52 fact that this estimate of the maximum wave speed is a guaranteed upper bound implies that the
 53 proposed numerical algorithm satisfies the invariant-domain properties stated in Theorem 4.6. The
 54 technique introduced in the paper is illustrated in §6 with continuous finite elements and various
 55 equations of states. Finally, the paper is supplemented with an appendix collecting technical results.
 56 Various pieces of software are made publicly available to guarantee reproducibility (Clayton et al.
 57 [3, 4]).

58 **2. Formulation of the problem.** We formulate the problem and introduce notation in this
 59 section. The main motivation for the theory developed in the paper is given at the end of §2.2.

60 **2.1. The Euler equations.** We consider a compressible inviscid fluid occupying a bounded,
 61 polyhedral domain D in \mathbb{R}^d . Here d is the space dimension. We assume that the dynamics of the
 62 system is modeled by the compressible Euler equations equipped with an equation of state that can
 63 be either tabulated or given by a very complicated analytic expression. The dependent variable is
 64 $\mathbf{u} := (\rho, \mathbf{m}, E)^\top \in \mathbb{R}^{d+2}$, where ρ is the density, \mathbf{m} the momentum, E the total mechanical energy.
 65 In this paper \mathbf{u} is considered to be a column vector. The velocity is given by $\mathbf{v} := \rho^{-1}\mathbf{m}$. The
 66 quantity $e(\mathbf{u}) := \rho^{-1}E - \frac{1}{2}\|\mathbf{v}\|_{\ell_2}^2$ is the specific internal energy. To simplify the notation later on we
 67 introduce the flux $\mathbf{f}(\mathbf{u}) := (\mathbf{m}, \mathbf{v} \otimes \mathbf{m} + p(\mathbf{u})\mathbb{I}_d, \mathbf{v}(E + p))^\top \in \mathbb{R}^{(d+2) \times d}$, where \mathbb{I}_d is the $d \times d$ identity
 68 matrix. The convention adopted in the paper is that for any vectors \mathbf{a}, \mathbf{b} , with entries $\{a_k\}_{k \in \{1:d\}}$,
 69 $\{b_k\}_{k \in \{1:d\}}$, the following holds: $(\mathbf{a} \otimes \mathbf{b})_{kl} = a_k b_l$ and $\nabla \cdot \mathbf{a} = \sum_{k \in \{1:d\}} \partial_{x_k} a_k$. Moreover, for any
 70 second-order tensor \mathbf{g} with entries $\{g_{kl}\}_{k \in \{1:d+2\}}^{l \in \{1:d\}}$, we define $(\nabla \cdot \mathbf{g})_k = \sum_{l \in \{1:d\}} \partial_{x_l} g_{kl}$.

71 Given some initial time t_0 and initial data $\mathbf{u}_0(\mathbf{x}) := (\rho_0, \mathbf{m}_0, E_0)(\mathbf{x})$, we look for $\mathbf{u}(\mathbf{x}, t) :=$
 72 $(\rho, \mathbf{m}, E)(\mathbf{x}, t)$ solving the following system in some weak sense:

$$73 \quad (2.1a) \quad \partial_t \rho + \nabla \cdot (\mathbf{v} \rho) = 0 \quad \text{a.e. } t > t_0, \mathbf{x} \in D,$$

$$74 \quad (2.1b) \quad \partial_t \mathbf{m} + \nabla \cdot (\mathbf{v} \otimes \mathbf{m} + p(\mathbf{u})\mathbb{I}_d) = \mathbf{0} \quad \text{a.e. } t > t_0, \mathbf{x} \in D,$$

$$75 \quad (2.1c) \quad \partial_t E + \nabla \cdot (\mathbf{v}(E + p(\mathbf{u}))) = 0 \quad \text{a.e. } t > t_0, \mathbf{x} \in D,$$

77 where $p : \mathcal{A} \rightarrow \mathbb{R}$ is the pressure, and \mathcal{A} is the admissible set:

$$78 \quad (2.2) \quad \mathcal{A} := \{\mathbf{u} = (\rho, \mathbf{m}, E) \in \mathbb{R}^{d+2} \mid \rho > 0, e(\mathbf{u}) > 0\}.$$

79 We refer to the mapping $p : \mathcal{A} \rightarrow \mathbb{R}$ as the *oracle*. For all $\beta \geq 0$, we introduce the following convex
 80 subset of \mathcal{A} :

$$81 \quad (2.3) \quad \mathcal{B}(\beta) := \{\mathbf{u} = (\rho, \mathbf{m}, E) \in \mathbb{R}^{d+2} \mid \rho > 0, 1 - \beta\rho > 0, e(\mathbf{u}) > 0\}.$$

82 We further assume in the paper that the oracle is such that there exists a number $b \geq 0$, henceforth
 83 called the covolume constant, so that the following holds for all $\mathbf{u} \in \mathcal{B}(b)$:

84 (2.4)
$$p(\mathbf{u}) > 0.$$

85 The inverse of the covolume constant b is the maximal density the fluid can reach. We take $b = 0$
 86 if this constant is not a priori known.

87 Our goal in the paper is to approximate (2.1) by adapting the technique described in Guer-
 88 mond and Popov [12]. As explained in the next section, this is done by constructing an artificial
 89 viscosity that ensures that some relevant invariant-domain properties can be established, thereby
 90 guaranteeing that the approximation technique is robust (i.e., satisfies physical bounds under a
 91 reasonable CFL condition). The two key difficulties that arise in this endeavor are that it is nearly
 92 impossible to construct solutions to elementary Riemann problems (or at least highly nontrivial,
 93 see e.g., Quartapelle et al. [24], Fossati and Quartapelle [9]), since the equation of state is either
 94 not available or too complicated. We propose a solution to this problem in §3 and §4. Taking
 95 inspiration from Colella and Glaz [5], Abgrall and Karni [1], Pantano et al. [22], we introduce a
 96 technique consisting of approximating the oracle by a covolume γ -law, where γ solves an additional
 97 conservation equation.

98 *Remark 2.1* (Pressure). In practice there are many equations of state that cannot guarantee
 99 (2.4) over the entire set $\mathcal{B}(b)$, but the algorithm proposed in the paper works properly as long as the
 100 numerical states stay in a subset of $\mathcal{B}(b)$ where the pressure stays positive. This situation occurs
 101 in many realistic applications. \square

102 **2.2. Space and time approximation.** Let us first recall the space and time approximation
 103 technique described in [12]. This method is in some sense a discretization-independent extension
 104 of the scheme by Lax [18, p. 163]. Without going into the details, we assume that we have at
 105 hand a fully discrete scheme where time is approximated by using the forward Euler time stepping
 106 and space is approximated by using some “centered” approximation of (2.1) (i.e., without any
 107 artificial viscosity to stabilize the approximation). We denote by t^n the current time, $n \in \mathbb{N}$, and
 108 we denote by τ the current time step size; that is $t^{n+1} := t^n + \tau$. Let us assume that the current
 109 approximation is a collection of states $\{\mathbf{U}_i^n\}_{i \in \mathcal{V}}$, where the index set \mathcal{V} is used to enumerate all
 110 the degrees of freedom of the approximation. Here $\mathbf{U}_i^n \in \mathbb{R}^{d+2}$ for all $i \in \mathcal{V}$. We assume that the
 111 centered update is given by $\mathbf{U}_i^{\text{G},n+1}$ with

112 (2.5)
$$\frac{m_i}{\tau}(\mathbf{U}_i^{\text{G},n+1} - \mathbf{U}_i^n) + \sum_{j \in \mathcal{G}(i)} \mathbb{f}(\mathbf{U}_j^n) \mathbf{c}_{ij} = \mathbf{0}.$$

113 The quantity m_i is called lumped mass and we assume that $m_i > 0$ for all $i \in \mathcal{V}$. The vector
 114 $\mathbf{c}_{ij} \in \mathbb{R}^d$ encodes the space discretization. The index set $\mathcal{G}(i)$ is called local stencil. This set
 115 collects only the degrees of freedom in \mathcal{V} that interact with i (i.e., $j \notin \mathcal{G}(i) \Rightarrow \mathbf{c}_{ij} = \mathbf{0}$). We view
 116 $\frac{1}{m_i} \sum_{j \in \mathcal{G}(i)} \mathbb{f}(\mathbf{U}_j^n) \mathbf{c}_{ij}$ as a Galerkin (or centered or inviscid) approximation of $\nabla \cdot \mathbb{f}(\mathbf{u})$ at time t^n at
 117 some grid point (or cell) $i \in \mathcal{V}$. The super-index G is meant to remind us that (2.5) is a Galerkin
 118 (or inviscid or centered) approximation of (2.1). That is, we assume that the consistency error
 119 in space in (2.5) scales optimally with respect to the meshsize for the considered approximation
 120 setting. We do not need to be more specific at this point. The only requirement that we make on

121 the coefficients \mathbf{c}_{ij} is that the method is conservative; that is to say, we assume that

$$122 \quad (2.6) \quad \mathbf{c}_{ij} = -\mathbf{c}_{ji} \quad \text{and} \quad \sum_{j \in \mathcal{G}(i)} \mathbf{c}_{ij} = \mathbf{0}.$$

123
124 An immediate consequence of this assumption is that the total mass is conserved: $\sum_{i \in \mathcal{V}} m_i \mathbf{U}_i^{\mathbf{G}, n+1} =$
125 $\sum_{i \in \mathcal{V}} m_i \mathbf{U}_i^n$. Notice that for every $i \in \mathcal{V}$, the update (2.5) invokes the oracle $\text{card}(\mathcal{G}(i))$ times,
126 because computing $\mathbb{f}(\mathbf{U}_j^n)$ requires computing $p(\mathbf{U}_j^n)$ for all $j \in \mathcal{G}(i)$.

127 *Remark 2.2* (literature). The reader is referred to [12, 13] for realizations of the algorithm (2.5)
128 with continuous finite elements. Realizations of the algorithm with discontinuous elements and
129 with finite volumes are described in [14]. \square

130 Of course, the approximation (2.5) is in general not appropriate if the solution to (2.1) is not
131 smooth. To recover some sort of stability (we are going to make a more precise stability statement
132 later in Theorem 4.6), we modify the scheme by adding an artificial graph viscosity based on the
133 stencil $\mathcal{G}(i)$; that is, we compute the stabilized update \mathbf{U}_i^{n+1} by setting:

$$134 \quad (2.7) \quad \frac{m_i}{\tau} (\mathbf{U}_i^{n+1} - \mathbf{U}_i^n) + \sum_{j \in \mathcal{G}(i)} \mathbb{f}(\mathbf{U}_j^n) \mathbf{c}_{ij} - \sum_{j \in \mathcal{G}(i) \setminus \{i\}} d_{ij}^n (\mathbf{U}_j^n - \mathbf{U}_i^n) = \mathbf{0}.$$

135 Here d_{ij}^n is the yet to be defined artificial graph viscosity. We assume that

$$136 \quad (2.8) \quad d_{ij}^n = d_{ji}^n > 0, \quad \text{if } i \neq j.$$

138 The symmetry assumption is essential for the method to be conservative. The question addressed
139 in the paper is the following: how large should d_{ij}^n be for the scheme to preserve invariant sets (and
140 possibly be entropy satisfying for some finite collection of entropies)?

141 One key observation is that one can rewrite (2.7) as follows:

$$142 \quad (2.9) \quad \mathbf{U}_i^{n+1} = \left(1 - \sum_{j \in \mathcal{G}(i) \setminus \{i\}} \frac{2\tau d_{ij}^n}{m_i} \right) \mathbf{U}_i^n + \sum_{j \in \mathcal{G}(i) \setminus \{i\}} \frac{2\tau d_{ij}^n}{m_i} \bar{\mathbf{U}}_{ij}^n,$$

144 with the auxiliary states $\bar{\mathbf{U}}_{ij}^n$ defined as follows:

$$145 \quad (2.10) \quad \bar{\mathbf{U}}_{ij}^n := \frac{1}{2} (\mathbf{U}_i^n + \mathbf{U}_j^n) - (\mathbb{f}(\mathbf{U}_j^n) - \mathbb{f}(\mathbf{U}_i^n)) \mathbf{n}_{ij} \frac{\|\mathbf{c}_{ij}\|_{\ell^2}}{2d_{ij}^n}.$$

147 Hence, if the time step is small enough, (2.9) shows that \mathbf{U}_i^{n+1} is a convex combination of the
148 following states $(\bar{\mathbf{U}}_{ij}^n)_{j \in \mathcal{G}(i)}$ (with the convention $\bar{\mathbf{U}}_{ii}^n := \mathbf{U}_i^n$). Hence if one can prove that the
149 auxiliary states $\bar{\mathbf{U}}_{ij}^n$ are in the set $\mathcal{B}(b)$ for all $j \in \mathcal{G}(i)$, then the update \mathbf{U}_i^{n+1} is also in $\mathcal{B}(b)$, thereby
150 establishing one important invariant-domain property. (Notice in passing that it is essential here
151 to assume $d_{ij}^n \neq 0$.)

152 The main objective of the paper is to describe a technique to estimate d_{ij}^n that guarantees that
153 $\bar{\mathbf{U}}_{ij}^n \in \mathcal{B}(b)$ provided both states \mathbf{U}_i^n and \mathbf{U}_j^n are in $\mathcal{B}(b)$. This is done by showing that $\bar{\mathbf{U}}_{ij}^n$ is a
154 space average of a solution to a Riemann problem, and by showing that this solution does satisfy
155 the invariant-domain property we are after. Then d_{ij}^n is defined so that $d_{ij}^n \geq \lambda_{ij, \max} \|\mathbf{c}_{ij}\|_{\ell^2}$, where
156 $\lambda_{ij, \max}$ is any upper bound on the maximum wave speed in the said Riemann problem.

157 **3. The extended Riemann problem.** An important step in [12] toward proving that the
 158 auxiliary state $\bar{\mathbf{U}}_{ij}^n$ defined in (2.10) is a “good” state, if $\lambda_{ij,\max}$ is an upper bound on the maximum
 159 wave speed in the Riemann problem, consists of realizing that in this case $\bar{\mathbf{U}}_{ij}^n$ is a space average
 160 of the exact solution to the one-dimensional Riemann problem with flux $\mathbb{f}(\mathbf{v})\mathbf{n}_{ij}$, left data \mathbf{U}_i , and
 161 right data \mathbf{U}_j . The main difficulty we are facing in the present situation is that there is no analytical
 162 way to estimate an upper bound $\lambda_{ij,\max}$ since the pressure is given by an oracle. We show in this
 163 section how to go around this difficulty.

164 **3.1. Extension of the system and 1D reduction.** To avoid having to refer to particular
 165 states \mathbf{U}_i^n and \mathbf{U}_j^n , we now assume that we are given a left and a right admissible states, \mathbf{u}_L and \mathbf{u}_R .
 166 We also denote \mathbf{n}_{ij} by \mathbf{n} . Instead of considering the Riemann problem where the pressure is given
 167 by the oracle, we now consider an extended Riemann problem. First we make a change of basis
 168 and introduce $\mathbf{t}_1, \dots, \mathbf{t}_{d-1}$ so that $\{\mathbf{n}, \mathbf{t}_1, \dots, \mathbf{t}_{d-1}\}$ forms an orthonormal basis of \mathbb{R}^d . With this
 169 new basis we have $\mathbf{m} = (m, \mathbf{m}^\perp)^\top$, where $m := \rho v$, $v := \mathbf{v} \cdot \mathbf{n}$, $\mathbf{m}^\perp := \rho(\mathbf{v} \cdot \mathbf{t}_1, \dots, \mathbf{v} \cdot \mathbf{t}_{d-1}) := \rho \mathbf{v}^\perp$.
 170 Second, we augment the system by introducing a new scalar variable Γ (and $\gamma := \frac{\Gamma}{\rho}$), the augmented
 171 state $\tilde{\mathbf{u}} := (\mathbf{u}, \Gamma)^\top$, and the extend the flux as follows:

$$172 \quad (3.1) \quad \tilde{\mathbb{f}}(\tilde{\mathbf{u}}) := (\mathbf{m}, \mathbf{v} \otimes \mathbf{m} + \tilde{p}(\tilde{\mathbf{u}})\mathbb{I}_d, \mathbf{v}(E + \tilde{p}(\tilde{\mathbf{u}})), \mathbf{v}\Gamma)^\top = (\mathbb{f}(\tilde{\mathbf{u}}), \mathbf{v}\Gamma)^\top,$$

173 with the new pressure

$$174 \quad (3.2) \quad \tilde{p}(\tilde{\mathbf{u}}) := \frac{(\Gamma - \rho)e(\mathbf{u})}{1 - b\rho} = (\gamma - 1)\frac{\rho e(\mathbf{u})}{1 - b\rho},$$

175 where $e(\mathbf{u}) := \frac{1}{\rho}(E - \frac{\|\mathbf{m}\|_{\ell^2}^2}{2\rho})$. Here b is either given to us because this parameter can be measured,
 176 or b is set to be zero if one does not have any a priori knowledge on the nature of the fluid. Notice
 177 that Γ is the last component of the extended variable $\tilde{\mathbf{u}}$; neither Γ nor $\gamma = \rho^{-1}\Gamma$ are assumed to be
 178 constant. The extended Riemann problem consists of seeking $\tilde{\mathbf{u}} := (\mathbf{u}, \Gamma)^\top = (\rho, \mathbf{m}, E, \Gamma)^\top$ so that

$$179 \quad (3.3) \quad \partial_t \tilde{\mathbf{u}} + \partial_x (\tilde{\mathbb{f}}(\tilde{\mathbf{u}})\mathbf{n}) = \mathbf{0}, \quad \tilde{\mathbf{u}} = \begin{pmatrix} \rho \\ m \\ \mathbf{m}^\perp \\ E \\ \Gamma \end{pmatrix}, \quad \tilde{\mathbb{f}}(\tilde{\mathbf{u}})\mathbf{n} = \begin{pmatrix} m \\ \frac{1}{\rho}m^2 + \tilde{p}(\tilde{\mathbf{u}}) \\ \mathbf{v}\mathbf{m}^\perp \\ \mathbf{v}(E + \tilde{p}(\tilde{\mathbf{u}})) \\ \mathbf{v}\Gamma \end{pmatrix},$$

180 with left data and right data $(\rho_Z, \mathbf{m}_Z \cdot \mathbf{n}, \mathbf{m}_Z^\perp, E_Z, \Gamma_Z)^\top$, where $Z \in \{L, R\}$, and Γ_Z is defined so
 181 that $\tilde{p}(\tilde{\mathbf{u}}_Z) = p(\mathbf{u}_Z) =: p_Z$, i.e., $\Gamma_Z := \rho_Z + \frac{p_Z(1 - b\rho_Z)}{e_Z}$, (notice that this means $\gamma_Z := 1 + \frac{p_Z(1 - b\rho_Z)}{\rho_Z e_Z}$).

182 As usually done in the literature, the above problem can be solved in two steps. First one solves

$$183 \quad (3.4) \quad \partial_t \begin{pmatrix} \rho \\ m \\ \mathcal{E} \\ \Gamma \end{pmatrix} + \partial_x \begin{pmatrix} m \\ \frac{1}{\rho}m^2 + p \\ \frac{m}{\rho}(\mathcal{E} + p) \\ \frac{m}{\rho}\Gamma \end{pmatrix} = \mathbf{0}, \quad \text{with } p(\rho, m, \mathcal{E}, \Gamma) := \frac{\gamma - 1}{1 - b\rho} \left(\mathcal{E} - \frac{m^2}{2\rho} \right),$$

184 with left data and right data $(\rho_Z, \mathbf{m}_Z \cdot \mathbf{n}, \mathcal{E}_Z, \Gamma_Z)^\top$, where $\mathcal{E} := E - \frac{\|\mathbf{m}^\perp\|_{\ell^2}^2}{2\rho}$. Notice in passing
 185 that $E - \frac{\|\mathbf{m}\|_{\ell^2}^2}{2\rho} = \mathcal{E} - \frac{m^2}{2\rho}$, i.e., the internal energy does not depend on the change of basis. This,

186 together with the definition of γ_Z , implies that $\rho_Z := \frac{\gamma_Z - 1}{1 - b\rho_Z}(\mathcal{E}_Z - \frac{m_Z^2}{2\rho_Z}) = \frac{\gamma_Z - 1}{1 - b\rho_Z}(E_Z - \frac{\|\mathbf{m}_Z\|_{\ell^2}^2}{2\rho_Z}) = p_Z$.
 187 Second, one obtains the full solution to the Riemann problem (3.3) by determining \mathbf{m}^\perp . This field
 188 is obtained by solving $\partial_t \mathbf{m}^\perp + \partial_x (\mathbf{v} \mathbf{m}^\perp) = 0$ with the appropriate left and right data. Just like
 189 in the case of the Euler equations, one never solves the second step since it does not affect the
 190 maximum wave speed and the structure of the Riemann problem. In the rest of this paper we
 191 solely focus our attention on the system (3.4).

192 *Remark 3.1* (Invariant domain properties). At this point, it is important to notice that
 193 $\tilde{\mathbf{f}}(\tilde{\mathbf{u}}_Z) = (\mathbf{f}(\mathbf{u}_Z), \mathbf{v}_Z \Gamma_Z)^\top$ because, as already mentioned above, $\tilde{p}(\tilde{\mathbf{u}}_Z) = p_Z = p(\mathbf{u}_Z)$. Then,
 194 recalling (2.10), and setting $\lambda := \frac{d_{ij}^n}{\|\mathbf{c}_{ij}\|_{\ell^2}}$ and $\bar{\mathbf{u}}_{LR} := \bar{\mathbf{U}}_{ij}$, the extended auxiliary state based on the
 195 extended flux $\tilde{\mathbf{f}}$, say $\bar{\tilde{\mathbf{u}}}_{LR}$, satisfies the following identity:

$$196 \quad (3.5) \quad \bar{\tilde{\mathbf{u}}}_{LR} = \left(\frac{1}{2}(\Gamma_L + \Gamma_R) - \frac{1}{2\lambda}(\mathbf{v}_R \Gamma_R - \mathbf{v}_L \Gamma_L) \cdot \mathbf{n} \right)$$

197 That is, the density, the momentum, and the total energy of the states $\bar{\tilde{\mathbf{u}}}_{LR}$ and $\bar{\mathbf{u}}_{LR}$ are identical.
 198 This implies that these two states have the same density and the same internal energy. As a result,
 199 if one can prove that the density and the internal energy of the state $\bar{\tilde{\mathbf{u}}}_{LR}$ are both positive, then
 200 this conclusion automatically carries over to the state $\bar{\mathbf{u}}_{LR}$. This remark is essential, and it is the
 201 main motivation for our introducing the extended Riemann problem. \square

202 **3.2. The invariant domain preserving properties.** We will use the technique of Lax con-
 203 sisting of piecing together elementary waves to construct a weak solution to the extended Riemann
 204 problem (3.4). We will show that this weak solution preserves positivity of the density and the
 205 internal energy (see Remark 3.1). We will also show that the local gamma constant is uniformly
 206 bounded from bellow: $\gamma \geq \min(\gamma_L, \gamma_R)$. The key tool we are going to invoke is the following lemma.

207 **LEMMA 3.2** (Riemann average). *Let m be a positive integer. Let \mathcal{A} be a subset of \mathbb{R}^m . Let*
 208 *$\mathbf{g} \in C^1(\mathcal{A}; \mathbb{R}^m)$ be a one-dimensional flux. Let $\mathbf{w}_L, \mathbf{w}_R \in \mathcal{A}$. Assume that the following Riemann*
 209 *problem*

$$210 \quad (3.6) \quad \partial_t \mathbf{w} + \partial_x \mathbf{g}(\mathbf{w}) = \mathbf{0}, \quad \mathbf{w}(x, 0) = \begin{cases} \mathbf{w}_L & x < 0, \\ \mathbf{w}_R & x > 0, \end{cases}$$

211 *has a weak solution \mathbf{w} in $L^\infty(\mathbb{R} \times (0, \infty); \mathbb{R}^m) \cap C^0([0, \infty); L^1_{\text{loc}}(\mathbb{R}; \mathbb{R}^m))$. Assume that this Riemann*
 212 *solution has a finite maximum wave speed (meaning, there exists $\lambda_{\max} > 0$ s.t. $\mathbf{w}(x, t) = \mathbf{w}_L$ if*
 213 *$x < -\lambda_{\max} t$ and $\mathbf{w}(x, t) = \mathbf{w}_R$ if $x > \lambda_{\max} t$.) Let \mathcal{B} be a convex subset of \mathcal{A} and assume that*
 214 *$\mathbf{w}(x, t) \in \mathcal{B}$ for a.e. $x \in \mathbb{R}$ and all $t > 0$. Let $\bar{\mathbf{w}} := \int_{-\frac{1}{2}}^{\frac{1}{2}} \mathbf{w}(x, t) dx$. Then the following holds true*
 215 *for all $t \in (0, \frac{1}{2\lambda_{\max}})$:*

216 (i) $\bar{\mathbf{w}}(t) = \frac{1}{2}(\mathbf{w}_L + \mathbf{w}_R) - (\mathbf{g}(\mathbf{w}_R) - \mathbf{g}(\mathbf{w}_L))t$;

217 (ii) $\bar{\mathbf{w}}(t) \in \mathcal{B}$;

218 (iii) Let $\Psi \in C^1(\mathcal{B}; \mathbb{R})$ be a quasiconcave functional. Assume that $\Psi(\mathbf{w}(x, t)) \geq 0$ for a.e. $x \in \mathbb{R}$
 219 and all $t > 0$. Then $\Psi(\bar{\mathbf{w}}(t)) \geq 0$.

220 (iv) Let $\Psi \in C^1(\mathcal{B}; \mathbb{R})$ be a concave functional. Assume that $\Psi(\mathbf{w}(x, t)) \geq 0$ for a.e. $x \in \mathbb{R}$ and all
 221 $t > 0$. Assume that there exists $\lambda_\flat, \lambda_\sharp \in [-\lambda_{\max}, \lambda_{\max}]$, $\lambda_\flat < \lambda_\sharp$, so that $\Psi(\mathbf{w}(x, t)) > 0$ for a.e.
 222 $\frac{x}{t} \in (\lambda_\flat, \lambda_\sharp)$. Then $\Psi(\bar{\mathbf{w}}(t)) > 0$.

223 *Proof.* (i) Let w_1, \dots, w_m be the m components of \mathbf{w} , and let g_1, \dots, g_m be the m components
 224 of the flux \mathbf{g} . Let $l \in \{1:m\}$. Since \mathbf{w} is a weak solution to (3.6), we have

$$225 \quad 0 = \int_{-\infty}^{\infty} \int_0^{\infty} (-w_l \partial_\tau \phi - g_l(\mathbf{w}) \partial_x \phi) \, d\tau \, dx - w_{l,L} \int_{-\infty}^0 \phi(x, 0) \, dx - w_{l,R} \int_0^{\infty} \phi(x, 0) \, dx$$

227 for all $\phi \in W^{1,\infty}(\mathbb{R} \times [0, \infty); \mathbb{R})$ with compact support in $\mathbb{R} \times [0, \infty)$. Here $w_{l,Z}$ is the l -th component
 228 of \mathbf{w}_Z . Now we define a sequence of smooth functions $(\phi_\epsilon)_{\epsilon>0}$ with $\phi_\epsilon(x, t) = \phi_{1,\epsilon}(|x|)\phi_{2,\epsilon}(\tau)$

$$229 \quad \phi_{1,\epsilon}(x) = \begin{cases} 1 & 0 \leq x \leq \frac{1}{2}, \\ \frac{1}{\epsilon}(-x + \frac{1}{2} + \epsilon) & \frac{1}{2} \leq x \leq \frac{1}{2} + \epsilon, \\ 0 & \frac{1}{2} + \epsilon \leq x, \end{cases} \quad \phi_{2,\epsilon}(\tau) = \begin{cases} 1 & 0 \leq \tau \leq t, \\ \frac{1}{\epsilon}(-\tau + t + \epsilon) & t \leq \tau \leq t + \epsilon, \\ 0 & t + \epsilon \leq \tau. \end{cases}$$

231 Using that $w_l \in C^0([0, \infty); L^1_{\text{loc}}(\mathbb{R}))$, we infer that $\int_{-\infty}^{\infty} \int_0^{\infty} -w_l \partial_\tau \phi_\epsilon \, dx \, d\tau \rightarrow \int_{-\frac{1}{2}}^{\frac{1}{2}} w_l(x, t) \, dx$ as $\epsilon \rightarrow$
 232 0. Likewise, we have $\int_{-\infty}^{\infty} \int_0^{\infty} -g_l(\mathbf{w}) \partial_x \phi_\epsilon \, dx \, d\tau \rightarrow \int_0^t (g_l(\mathbf{w}_R) - g_l(\mathbf{w}_L)) \, d\tau = (g_l(\mathbf{w}_R) - g_l(\mathbf{w}_L))t$
 233 as $\epsilon \rightarrow 0$. Finally, $-w_{l,L} \int_{-\infty}^0 \phi_\epsilon(x, 0) \, dx - w_{l,R} \int_0^{\infty} \phi_\epsilon(x, 0) \, dx \rightarrow -\frac{1}{2}(w_{l,L} + w_{l,R})$ as $\epsilon \rightarrow 0$. In
 234 conclusion, we have established that

$$235 \quad 0 = \bar{\mathbf{w}}(t) + (\mathbf{g}(\mathbf{w}_R) - \mathbf{g}(\mathbf{w}_L))t - \frac{1}{2}(\mathbf{w}_L + \mathbf{w}_R).$$

236 (ii) Since \mathcal{B} is convex, $\mathbf{w}(x, t) \in \mathcal{B}$ for a.e. $x \in \mathbb{R}$ and all $t > 0$, and the length of the interval $[-\frac{1}{2}, \frac{1}{2}]$
 237 is 1, we infer that $\bar{\mathbf{w}}(t) \in \mathcal{B}$.

238 (iii) Let $\Psi \in C^1(\mathcal{B}; \mathbb{R})$ be a quasiconcave functional. The quasiconcavity implies that $\Psi(\bar{\mathbf{w}}(t)) \geq$
 239 $\text{ess inf}_{x \in (-\frac{1}{2}, \frac{1}{2})} \Psi(\mathbf{w}(x, t)) \geq 0$.

240 (iv) Let $\Psi \in C^1(\mathcal{B}; \mathbb{R})$ be a concave functional. Jensen's inequality implies

$$241 \quad \Psi(\bar{\mathbf{w}}(t)) \geq \int_{-\frac{1}{2}}^{\frac{1}{2}} \Psi(\mathbf{w}(x, t)) \, dx \geq \int_{\lambda_b t}^{\lambda_\sharp t} \Psi(\mathbf{w}(x, t)) \, dx > 0,$$

242 where we used $-\frac{1}{2} \leq \lambda_b t < \lambda_\sharp t \leq \frac{1}{2}$. This concludes the proof. \square

243 *Remark 3.3* (Weak solution). Notice that Lemma 3.2 only requires us to have access to a weak
 244 solution of (3.6) that satisfies an invariant-domain property (i.e., $\mathbf{w}(x, t) \in \mathcal{B}$ for a.e. $x \in \mathbb{R}$ and all
 245 $t > 0$). No entropy inequality or additional smoothness condition is needed. \square

246 **4. Solution of the extended Riemann problem.** We now construct a weak solution to
 247 the extended Riemann problem (3.4) using the technique described in Lax [19] (we also refer to
 248 Holden and Risebro [15, Chap. 5], Godlewski and Raviart [10, Chap. 1], Toro [27, Chap. 4] for
 249 further details on the Riemann problem). No originality is claimed on this construction, but we
 250 give the details for completeness.

251 **4.1. Definition of the star states.** We first notice that the Jacobian matrix of (3.4) is
 252 diagonalizable and has three distinct eigenvalues. The eigenvalue $\frac{m}{\rho}$ has multiplicity 2. Then, as
 253 usual, we postulate that the solution to (3.4) is self-similar and composed of three waves hereafter
 254 called L-wave, C-wave, and R-wave. The L-wave and the R-wave are either shocks or expansions.
 255 The L-wave will be generated using the covolume equation of state with γ_L and the R-wave will be
 256 generated by using the covolume equation of state with γ_R . The C-wave is a contact discontinuity

257 for the density and Γ . Compared to the technique described in Toro [27, Chap. 4], the only new
 258 feature here is that the dependent variable has a fourth component Γ . The purpose of this section
 259 is to introduce quantities that are useful to define the three waves in question: the intermediate
 260 densities ρ_L^* , ρ_R^* , the intermediate velocities v_L^* , v_R^* , v^* , and the intermediate pressure p^* . The
 261 actual construction of the solution is done in §4.2 and §4.3.

262 In the rest of this section we use the primitive variables: density ρ , velocity v , pressure p , and
 263 $\gamma := \Gamma/\rho$. We use the symbol p to denote the pressure defined in (3.4). Notice that the oracle is
 264 only invoked to compute the two states p_L and p_R . We define the primitive state $\mathbf{c} := (\rho, v, p, \gamma)^\top$
 265 and set $\mathbf{c}_Z := (\rho_Z, v_Z, p_Z, \gamma_Z)^\top$. Recalling that we have defined $\gamma_Z := 1 + \frac{p_Z(1-b\rho_Z)}{\rho_Z e_Z}$, the oracle
 266 assumption (2.4) implies that $\min(\gamma_L, \gamma_R) > 1$.

267 We define the covolume sound speed $a_Z := \sqrt{\frac{\gamma_Z p_Z}{\rho_Z(1-b\rho_Z)}}$, the parameters $A_Z := \frac{2(1-b\rho_Z)}{(\gamma_Z+1)\rho_Z}$ and
 268 $B_Z := \frac{\gamma_Z-1}{\gamma_Z+1}p_Z$ corresponding to the Z state (see e.g., Toro [27, §4.7], [11]), and introduce the
 269 following function

$$270 \quad (4.1) \quad f_Z(p) := \begin{cases} f_Z^R(p) := \frac{2a_Z(1-b\rho_Z)}{\gamma_Z-1} \left(\left(\frac{p}{p_Z} \right)^{\frac{\gamma_Z-1}{2\gamma_Z}} - 1 \right) & \text{if } 0 \leq p < p_Z, \\ f_Z^S(p) := (p - p_Z) \left(\frac{A_Z}{p+B_Z} \right)^{\frac{1}{2}} & \text{if } p_Z \leq p. \end{cases}$$

271 The definition of $f_Z(p)$ makes sense because $1 < \gamma_Z$ and $0 \leq B_Z$. It is shown in Toro [27, §4.3.1]
 272 that the function $f_Z(p)$ is in $C^2(\mathbb{R}_+; \mathbb{R})$, monotone increasing, and concave.

273 We also define the function $\phi \in C^2(\mathbb{R}_+; \mathbb{R})$,

$$274 \quad (4.2) \quad \phi(p) := f_L(p) + f_R(p) + v_R - v_L, \quad p \in [0, \infty).$$

275 Notice in passing that assuming $\phi(0) < 0$ is equivalent to assuming that the following holds true:

$$276 \quad (4.3) \quad v_R - v_L < \frac{2a_L(1-b\rho_L)}{\gamma_L-1} + \frac{2a_R(1-b\rho_R)}{\gamma_R-1}.$$

277 This condition is known in the literature as the non-vacuum condition (see Toro [27, (4.40), p. 127]).

278 LEMMA 4.1. *If (4.3) holds, then ϕ has a unique positive root p^* .*

279 *Proof.* Since $\phi(0) = v_R - v_L - \frac{2a_L(1-b\rho_L)}{\gamma_L-1} - \frac{2a_R(1-b\rho_R)}{\gamma_R-1}$, the assumption (4.3) means that $\phi(0) < 0$.
 280 We then conclude that ϕ has a unique positive root since $\phi(p) \in C^2(\mathbb{R}_+; \mathbb{R})$ is strictly monotone
 281 increasing (and concave).

282 DEFINITION 4.2 (p^* , ρ_L^* , ρ_R^* , v_L^* , v_R^* , v^*). (i) *If the non-vacuum condition (4.3) holds, we*
 283 *denote by p^* the unique root of ϕ , and we set $v_L^* := v_L - f_L(p^*)$, $v_R^* := v_R + f_R(p^*)$, $v^* := v_L^* = v_R^*$.
 284 (ii) *If instead there is vacuum, we define $p^* := 0$ and set $v_L^* := v_L - f_L(0)$, $v_R^* := v_R + f_R(0)$.
 285 (iii) *We set $\rho_L^* = \rho_R^* = 0$ if $p^* = 0$; otherwise we set $\rho_Z^* := \left(b + \frac{1-b\rho_Z}{\rho_Z} \left(\frac{p_Z}{p^*} \right)^{\frac{1}{\gamma_Z}} \right)^{-1}$, $Z \in \{L, R\}$.***

286 Notice that the definition of v^* makes sense if the non-vacuum condition (4.3) holds since in
 287 this case $\phi(p^*) = 0 = v_R^* - v_L^*$. The definition of ρ_Z^* is continuous with respect to p^* , including at
 288 $p^* = 0$. To fully describe our weak solution, we introduce the following wave speeds:

$$289 \quad \lambda_L^-(p^*) := v_L - a_L \left(1 + \frac{\gamma_L + 1}{2\gamma_L} \left(\frac{p^* - p_L}{p_L} \right)_+ \right)^{\frac{1}{2}},$$

290

291

$$\lambda_L^+(p^*) := \begin{cases} v_L - f_L(p^*) - a_L \frac{1-b\rho_L}{1-b\rho_L^*} \left(\frac{p^*}{p_L}\right)^{\frac{\gamma_L-1}{2\gamma_L}} & \text{if } p^* < p_L, \\ \lambda_L^-(p^*) & \text{if } p_L \leq p^*, \end{cases}$$

292

$$\lambda_R^+(p^*) := v_R + a_R \left(1 + \frac{\gamma_R + 1}{2\gamma_R} \left(\frac{p^* - p_R}{p_R}\right)_+\right)^{\frac{1}{2}},$$

293

294

$$\lambda_R^-(p^*) := \begin{cases} v_R + f_R(p^*) + a_R \frac{1-b\rho_R}{1-b\rho_R^*} \left(\frac{p^*}{p_R}\right)^{\frac{\gamma_R-1}{2\gamma_R}} & \text{if } p^* < p_R, \\ \lambda_R^+(p^*) & \text{if } p_R \leq p^*, \end{cases}$$

295

296

LEMMA 4.3 (wave speeds). *Assume $1 < \min(\gamma_L, \gamma_R)$ and $0 < a_L, a_R$. Then, the following holds true:*

297

$$(4.4) \quad \lambda_L^-(p^*) \leq \lambda_L^+(p^*) \leq v_L^* \leq v_R^* \leq \lambda_R^-(p^*) \leq \lambda_R^+(p^*).$$

298

299

Proof. We will only consider the case $Z = L$; the case $Z = R$ is analogous. There are two possibilities: either $p^* < p_L$ or $p_L \leq p^*$. In the first case, $p^* < p_L$, we have

300

$$\lambda_L^-(p^*) = v_L - a_L < \lambda_L^+(p^*) = v_L - f_L(p^*) - a_L \frac{1-b\rho_L}{1-b\rho_L^*} \left(\frac{p^*}{p_L}\right)^{\frac{\gamma_L-1}{2\gamma_L}} \leq v_L - f_L(p^*) = v_L^*,$$

301

302

where we used above that $f_L(p^*) < 0$, $1 < \gamma_L$, $0 < a_L$, $\rho_L^* < \rho_L$, $0 \leq p^* < p_L$ and $0 < \frac{1-b\rho_L}{1-b\rho_L^*} \leq 1$.

In the second case, $p_L \leq p^*$, we have

303

$$\lambda_L^-(p^*) = \lambda_L^+(p^*) = v_L - a_L \left(1 + \frac{\gamma_L + 1}{2\gamma_L} \left(\frac{p^* - p_L}{p_L}\right)\right)^{\frac{1}{2}}$$

304

and

305

$$v_L^* = v_L - f_L(p^*) = v_L - (p^* - p_L) \left(\frac{A_L}{p^* + B_L}\right)^{\frac{1}{2}}.$$

306

Then proving the inequality $\lambda_L^+(p^*) < v_L^*$ is equivalent to showing that

307

$$\left(\frac{p^*}{p_L} - 1\right) \left(\frac{2(1-b\rho_L)}{\gamma_L(\gamma_L+1)} \frac{\gamma_L p_L}{\rho_L} \frac{1}{\frac{p^*}{p_L} + \frac{\gamma_L-1}{\gamma_L+1}}\right)^{\frac{1}{2}} < a_L \left(1 + \frac{\gamma_L + 1}{2\gamma_L} \left(\frac{p^* - p_L}{p_L}\right)\right)^{\frac{1}{2}}.$$

308

309

Using the substitution $x := \frac{p^*}{p_L} - 1$ and that $a_L := \sqrt{\frac{\gamma_L p_L}{\rho_L(1-b\rho_L)}}$, we derive that the above inequality is equivalent to proving that

310

$$\left(\frac{2}{\gamma_L(\gamma_L+1)}\right)^{\frac{1}{2}} x(1-b\rho_L) < \left(\left(x + \frac{2\gamma_L}{\gamma_L+1}\right)\left(\frac{\gamma_L+1}{2\gamma_L}x + 1\right)\right)^{\frac{1}{2}}$$

311

312

where $x > 0$. Squaring both sides, and recalling that $x > 0$, we observe that the above is equivalent to the inequality

313

$$0 < \left(\frac{\gamma_L+1}{2\gamma_L} - \frac{2(1-b\rho_L)^2}{\gamma_L(\gamma_L+1)}\right)x^2 + 2x + \frac{2\gamma_L}{\gamma_L+1}.$$

314

This inequality holds true for all $x \geq 0$ since we assumed that $1 < \gamma_L$ and $0 \leq 1 - b\rho_L \leq 1$. \square

315 **4.2. Definition of the L-wave and R-wave without vacuum.** We assume in this section
 316 that the non-vacuum condition (4.3) holds. The main result of this section is Lemma 4.4. The
 317 solution with vacuum is given in §4.3.

318 Recalling the notation from Definition 4.2, the proposed solution to (3.4) is self-similar and has
 319 the following form:

$$320 \quad (4.5) \quad \mathbf{c}(x, t) := \begin{cases} \mathbf{c}_L & \text{if } \frac{x}{t} < \lambda_L^-, \\ \mathbf{c}_{LL}(\frac{x}{t}) & \text{if } \lambda_L^- \leq \frac{x}{t} < \lambda_L^+, \\ \mathbf{c}_L^* & \text{if } \lambda_L^+ \leq \frac{x}{t} < v^*, \\ \mathbf{c}_R^* & \text{if } v^* \leq \frac{x}{t} < \lambda_R^-, \\ \mathbf{c}_{RR}(\frac{x}{t}) & \text{if } \lambda_R^- \leq \frac{x}{t} < \lambda_R^+, \\ \mathbf{c}_R & \text{if } \lambda_R^+ \leq \frac{x}{t}. \end{cases}$$

321 with $\mathbf{c}_L^* := (\rho_L^*, v^*, p^*, \gamma_L)^\top$ and $\mathbf{c}_R^* := (\rho_R^*, v^*, p^*, \gamma_R)^\top$. The parameters p^* , v^* , ρ_L^* , and ρ_R^* are
 322 defined in Definition 4.2. The two functions \mathbf{c}_{LL} , \mathbf{c}_{RR} are going to be defined to make sure that
 323 (4.5) is indeed a weak solution to (3.4). Notice that \mathbf{c} is uniquely defined owing to Lemma 4.3 (i.e.,
 324 the waves are well ordered).

325 Let us first construct the L-wave, i.e., we construct the function $\mathbf{c}_{LL}(\xi)$ where $\lambda_L^- \leq \xi < \lambda_L^+$.
 326 If $p_L \leq p^*$, then $\lambda_L^-(p^*) = \lambda_L^+(p^*)$ and the L-wave is a shock. In this case one does not need to
 327 define \mathbf{c}_{LL} since the interval $[\lambda_L^-, \lambda_L^+]$ is empty. If $p^* < p_L$, we postulate that the γ -component of
 328 \mathbf{c}_{LL} is constant and equal to γ_L . This means that the L-wave can be computed by assuming that
 329 the equation of state is a standard co-volume γ -law $\rho(1 - b\rho) = (\gamma_L - 1)\rho e$ (with $e = \frac{1}{\rho}(\mathcal{E} - \frac{m^2}{2\rho})$).
 330 In this case the L-wave is an expansion. The construction of this wave is well established, we refer
 331 for instance to Toro [27, Chap. 4]. More precisely, the self-similarity parameter $\xi = \frac{x}{t}$ (which is the
 332 eigenvalue of the Jacobian of the flux, $v - a$) can be expressed in terms of the parameter p :

$$333 \quad (4.6) \quad \xi_L(p) := v_L - f_L(p) - a_L \frac{1 - b\rho_L}{1 - b\rho(p)} \left(\frac{p}{p_L} \right)^{\frac{\gamma_L - 1}{2\gamma_L}}, \quad p \in [p^*, p_L],$$

334 where $\rho(p)$ is defined as follows:

$$335 \quad \frac{1}{\rho(p)} - b := \left(\frac{1}{\rho_L} - b \right) \left(\frac{p_L}{p} \right)^{\frac{1}{\gamma_L}}.$$

336 To simplify the notation we use the symbol $\xi(p)$ instead of $\xi_L(p)$ when the context is unambiguous.
 337 Notice in passing that $\lambda_L^-(p^*) = \xi(p_L)$ and $\lambda_L^+(p^*) = \xi(p^*)$. Since the function ξ is strictly decreasing
 338 in the interval $p \in [p^*, p_L]$, the inverse function theorem implies that p can be uniquely expressed
 339 in terms of ξ . We abuse the notation and denote by $p(\xi)$ the inverse function. Over the interval
 340 $\xi \in [\xi(p_L), \xi(p^*)] = [\lambda_L^-(p^*), \lambda_L^+(p^*)]$, we have (see Toro [27, §4.7.1])

$$341 \quad (4.7) \quad \mathbf{c}_{LL}(\xi) := \left(\rho_L \left(b\rho_L + (1 - b\rho_L) \left(\frac{p_L}{p(\xi)} \right)^{\frac{1}{\gamma_L}} \right)^{-1}, v_L - f_L(p(\xi)), p(\xi), \gamma_L \right)^\top.$$

342 Now we define \mathbf{c}_L^* . If $p^* < p_L$, the L-wave is an expansion and \mathbf{c}_L^* is defined to be the end point
 343 of the L-wave: $\mathbf{c}_L^* := \mathbf{c}_{LL}(\xi(p^*))$. If $p_L \leq p^*$, the L-wave is a shock. We still postulate that the

344 γ -component of \mathbf{c} is equal to γ_L for $\frac{x}{t} \leq \lambda_L^+(p^*)$. In this case we define \mathbf{c}_L^* so that the Rankine–
 345 Hugoniot relation holds between the two state \mathbf{c}_L and \mathbf{c}_L^* (see Toro [27, §4.7.1]). In conclusion, we
 346 have

$$347 \quad (4.8) \quad \mathbf{c}_L^* := \begin{cases} \mathbf{c}_{LL}(\xi(p^*)) & \text{if } p^* < p_L, \\ \left(\frac{\rho_L \left(\frac{p^*}{p_L} + \frac{\gamma_L - 1}{\gamma_L + 1} \right)}{\frac{\gamma_L - 1 + 2b\rho_L}{\gamma_L + 1} \frac{p^*}{p_L} + \frac{\gamma_L + 1 - 2b\rho_L}{\gamma_L + 1}}, v_L - f_L(p^*), p^*, \gamma_L \right)^\top & \text{if } p_L \leq p^*. \end{cases}$$

348 We define $\mathbf{c}_{RR}(\xi)$ similarly. If $p^* < p_R$, the R-wave is an expansion, otherwise it is a shock.
 349 Assuming that $p^* < p_R$, the self-similarity parameter $\xi = \frac{x}{t}$ can be expressed in terms of the
 350 parameter $p \in [p^*, p_R]$:

$$351 \quad (4.9) \quad \xi_R(p) := v_R + f_R(p) + a_R \frac{1 - b\rho_R}{1 - b\rho(p)} \left(\frac{p}{p_R} \right)^{\frac{\gamma_R - 1}{2\gamma_R}}$$

352 where we have defined

$$353 \quad \frac{1}{\rho(p)} - b := \left(\frac{1}{\rho_R} - b \right) \left(\frac{p_R}{p} \right)^{\frac{1}{\gamma_R}}.$$

354 To simplify the notation we use the symbol $\xi(p)$ instead of $\xi_R(p)$ when the context is unambiguous.
 355 Notice that in this case $\lambda_R^- = \xi(p^*)$, $\lambda_R^+ = \xi(p_R)$, and ξ is a strictly increasing function over the
 356 interval $[p^*, p_R]$. Over the interval $\xi \in [\xi(p^*), \xi(p_R)]$, we have

$$357 \quad (4.10) \quad \mathbf{c}_{RR}(\xi) := \left(\rho_R \left(b\rho_R + (1 - b\rho_R) \left(\frac{p_R}{p(\xi)} \right)^{\frac{1}{\gamma_R}} \right)^{-1}, v_R + f_R(p(\xi)), p(\xi), \gamma_R \right)^\top.$$

358 Now we define \mathbf{c}_R^* . If $p^* < p_R$, the R-wave is an expansion and \mathbf{c}_R^* is defined to be the end
 359 point of the wave: $\mathbf{c}_R^* = \mathbf{c}_{RR}(\xi(p^*))$. If $p_R \leq p^*$, the R-wave is a shock. We still postulate that
 360 the γ -component of \mathbf{c} is equal to γ_R for $v^* \leq \frac{x}{t} < \lambda_R^+$. In this case we define \mathbf{c}_R^* so that the
 361 Rankine–Hugoniot relation holds between the two state \mathbf{c}_R and \mathbf{c}_R^* . In conclusion, we have

$$362 \quad (4.11) \quad \mathbf{c}_R^* = \begin{cases} \mathbf{c}_{RR}(\xi(p^*)) & \text{if } p^* < p_R, \\ \left(\frac{\rho_R \left(\frac{p^*}{p_R} + \frac{\gamma_R - 1}{\gamma_R + 1} \right)}{\frac{\gamma_R - 1 + 2b\rho_R}{\gamma_R + 1} \frac{p^*}{p_R} + \frac{\gamma_R + 1 - 2b\rho_R}{\gamma_R + 1}}, v_R + f_R(p^*), p^*, \gamma_R \right)^\top & \text{if } p_R \leq p^*. \end{cases}$$

363 The key result of this section is summarized in the following Lemma.

364 LEMMA 4.4. *Assume that the non-vacuum condition (4.3) holds. The field $(\rho, \mathbf{m}, E, \Gamma)^\top$ defined
 365 by (4.5) is a weak solution to (3.4).*

366 *Proof.* In the domain $\{x < v^*t\}$, we have $\gamma = \gamma_L$; hence, $\Gamma = \gamma_L \rho$. This implies that the
 367 last equation in (3.4) is equivalent to the first equation (the conservation of mass). Moreover,
 368 the first three equations in (3.4) hold true in the weak sense since the field (ρ, m, \mathcal{E}) defined in
 369 (4.5) is by construction a weak solution to the regular Euler equations with the pressure law
 370 $p(1 - b\rho) := (\gamma_L - 1) \left(\mathcal{E} - \frac{m^2}{2\rho} \right)$.

371 Similarly, in the domain $\{x > v^*t\}$, we have $\gamma = \gamma_R$; hence, $\Gamma = \gamma_R \rho$ and the last equation
 372 in (3.4) is equivalent to the the conservation of mass equation. The first three equations in (3.4)

373 hold true in the weak sense because the field (ρ, m, \mathcal{E}) defined in (4.5) is by construction a weak
374 solution to the regular Euler equations with a pressure law $p(1 - b\rho) := (\gamma_R - 1) \left(\mathcal{E} - \frac{m^2}{2\rho} \right)$.

375 To be able to conclude the proof, we now have to make sure that the two states that are
376 separated by the line $\{x = v^*t\}$ satisfy the Rankine–Hugoniot relation. Let $\mathbf{c}_L^* = (\rho_L^*, v_L^*, p_L^*, \gamma_L^*)$
377 and $\mathbf{c}_R^* = (\rho_R^*, v_R^*, p_R^*, \gamma_R^*)$ be the two constant states defined above. Recall that the construction of
378 \mathbf{c}_L^* and \mathbf{c}_R^* is such that that $p_L^* = p_R^* = p^*$ (see (4.8) and (4.11)). We have to show that

$$\begin{aligned} 379 \quad & \rho_L^* v_L^* - \rho_R^* v_R^* = v^* (\rho_L^* - \rho_R^*) \\ 380 \quad & \rho_L^* (v_L^*)^2 + p_L^* - \rho_R^* (v_R^*)^2 - p_R^* = v^* (\rho_L^* v_L^* - \rho_R^* v_R^*) \\ 381 \quad & v_L^* (E_L^* - p_L^*) - v_R^* (E_R^* - p_R^*) = v^* (E_L^* - E_R^*), \\ 382 \quad & v_L^* \gamma_L - v_R^* \gamma_R = v^* (\gamma_L - \gamma_R). \end{aligned}$$

384 Since the non-vacuum condition (4.3) holds, we have $v^* := v_L^* = v_R^*$ (see Definition 4.2). Then it
385 follows that the above four equations indeed hold true. Therefore the field defined in (4.5) is a weak
386 solution to (3.4). \square

387 **4.3. Definition of the L-wave and R-wave when vacuum is present.** When (4.3) fails,
388 the solution contains a vacuum state. In this case both the L-wave and the R-waves are expansions.
389 Recall that in Definition 4.2 we have set

$$(4.12) \quad p^* := 0, \quad v_L^* := v_L - f_L(0) = v_L + \frac{2a_L(1 - b\rho_L)}{\gamma_L - 1}, \quad v_R^* := v_R + f_R(0) = v_R - \frac{2a_R(1 - b\rho_R)}{\gamma_R - 1}.$$

391 The solution to the extended Riemann problem (3.4) we propose is as follows:

$$(4.13) \quad \mathbf{c}(x, t) = \begin{cases} \mathbf{c}_L & \text{if } \frac{x}{t} < v_L - a_L, \\ \mathbf{c}_{LL}(\frac{x}{t}) & \text{if } \lambda_L^- \leq \frac{x}{t} < v_L^*, \\ \frac{v_R^* - \frac{x}{t}}{v_R^* - v_L^*} \mathbf{c}_L^* + \frac{\frac{x}{t} - v_L^*}{v_R^* - v_L^*} \mathbf{c}_R^* & \text{if } v_L^* \leq \frac{x}{t} < v_R^*, \\ \mathbf{c}_{RR}(\frac{x}{t}) & \text{if } v_R^* \leq \frac{x}{t} < v_R + a_R, \\ \mathbf{c}_R & \text{if } v_R + a_R \leq \frac{x}{t}. \end{cases}$$

393 The definitions of the expansion waves \mathbf{c}_{LL} and \mathbf{c}_{RR} are the same as in the non-vacuum case.
394 We define the states \mathbf{c}_L^* and \mathbf{c}_R^* as in §4.2 by setting $\mathbf{c}_L^* := \mathbf{c}_{LL}(v_L^*) = (0, v_L^*, 0, \gamma_L)^T$ and $\mathbf{c}_R^* :=$
395 $\mathbf{c}_{RR}(v_R^*) = (0, v_R^*, 0, \gamma_R)^T$. The key result of this section is the following Lemma.

396 **LEMMA 4.5.** *Assume that the vacuum condition holds, i.e., $p^* = 0$. The field $(\rho, \mathbf{m}, E, \Gamma)^T$*
397 *defined by (4.13) is a weak solution to (3.4).*

398 *Proof.* We have already established that, once expressed in conserved variable, (4.13) is a weak
399 solution to (3.4) in the regions $\{x < v_L^*t\} \cup \{v_R^*t < x\}$. In the region $\{v_L^*t < x < v_R^*t\}$, all the
400 conserved variables are zero by construction. Hence, (4.13) rewritten in conserved variables is also
401 weak solution to (3.4) in the region $\{v_L^*t < x < v_R^*t\}$. Let us verify now that the field defined
402 in (4.13) is continuous across the line $\{x = v_L^*t\}$. Denoting $\xi_L(p)$ the function defined in (4.6), we
403 obtain $\xi_L(0) = v_L - f_L(0) =: v_L^*$, i.e., $p(v_L^*) = 0$. Hence $\lim_{\xi \uparrow v_L^*} \mathbf{c}_{LL}(\xi) = (0, v_L^*, 0, \gamma_L)$. Moreover,
404 $\lim_{\xi \downarrow v_L^*} \frac{v_R^* - \xi}{v_R^* - v_L^*} \mathbf{c}_L^* + \frac{\xi - v_L^*}{v_R^* - v_L^*} \mathbf{c}_R^* = (0, v_L^*, 0, \gamma_L)$. This proves the assertion. This in turn establishes
405 that the conserved field is also continuous across $\{x = v_L^*t\}$. The argument to prove continuity
406 across $\{x = v_R^*t\}$ is similar. The conclusion follows readily. \square

407 **4.4. Summary.** In Sections §4.2 and §4.3 we have defined a weak solution to the extended
 408 Riemann problem (3.4). Notice that this weak solution satisfies the assumption of Lemma 3.2,
 409 i.e., it is in $L^\infty(\mathbb{R} \times (0, \infty); \mathbb{R}^m) \cap C^0([0, \infty); L^1_{\text{loc}}(\mathbb{R}; \mathbb{R}^m))$ with $m = d + 2$, and the maximum wave
 410 speed $\lambda_{\max} = \max(|\lambda_L^-(p^*)|, |\lambda_R^+(p^*)|) = \max(-\lambda_L^-(p^*), \lambda_R^+(p^*))$ is finite. As a result, we can invoke
 411 Lemma 3.2 for any quasiconcave functional. The following theorem is the main result of §4.

412 **THEOREM 4.6.** (i) Let $\mathbf{U}_i^n, \mathbf{U}_j^n$ be two states in $\mathcal{B}(b)$ (with $\mathcal{B}(b)$ defined in (2.3)). Let p^* be
 413 defined as in Definition 4.2 with left state \mathbf{U}_i^n and right state \mathbf{U}_j^n . Let \widehat{p}^* be any upper bound on p^*
 414 (i.e., $\widehat{p}^* \geq p^*$). Let

$$415 \quad (4.14a) \quad \widehat{\lambda}(\mathbf{n}_{ij}, \mathbf{U}_i^n, \mathbf{U}_j^n) := \max(-\lambda_L^-(\widehat{p}^*), \lambda_R^+(\widehat{p}^*)),$$

$$416 \quad (4.14b) \quad d_{ij}^n := \max(\widehat{\lambda}(\mathbf{n}_{ij}, \mathbf{U}_i^n, \mathbf{U}_j^n) \|\mathbf{c}_{ij}\|_{\ell^2}, \widehat{\lambda}(\mathbf{n}_{ji}, \mathbf{U}_j^n, \mathbf{U}_i^n) \|\mathbf{c}_{ji}\|_{\ell^2}).$$

418 Let $\overline{\mathbf{U}}_{ij}^n$ be defined by (2.10). Then $\overline{\mathbf{U}}_{ij}^n \in \mathcal{B}(b)$.

419 (ii) Let $i \in \mathcal{V}$. Assume that $\mathbf{U}_j^n \in \mathcal{B}(b)$ for all $j \in \mathcal{G}(i)$. Assume that d_{ij}^n is defined as above in
 420 (4.14b) for all $j \in \mathcal{G}(i)$. Assume that τ is small enough so that $\tau \sum_{j \in \mathcal{G}(i) \setminus \{i\}} \frac{2d_{ij}^n}{m_i} \leq 1$. Let \mathbf{U}_i^{n+1} be
 421 the update defined in (2.7). Then $\mathbf{U}_i^{n+1} \in \text{Conv}\{\overline{\mathbf{U}}_{ij}^n \mid j \in \mathcal{G}(i)\} \subset \mathcal{B}(b)$.

422 *Proof.* (i) We first notice that $\widehat{\lambda}(\mathbf{n}_{ij}, \mathbf{U}_i^n, \mathbf{U}_j^n) \geq \max(-\lambda_L^-(p^*), \lambda_R^+(p^*)) =: \lambda_{\max}$ since the func-
 423 tions $-\lambda_L^-$ and λ_R^+ are monotone increasing and $\widehat{p}^* \geq p^*$. We now apply Lemma 3.2 with the flux
 424 $\mathbf{g}(\tilde{\mathbf{w}}) = \tilde{\mathbf{f}}(\tilde{\mathbf{w}})\mathbf{n}$ and the Riemann data $\tilde{\mathbf{U}}_i^n, \tilde{\mathbf{U}}_j^n$. We observe that the Riemann solution defined in
 425 (4.5) and (4.13) has nonnegative density and nonnegative internal energy (recall that the internal
 426 energy ρe is equal to $\frac{1}{(\gamma-1)}(1-b\rho)p$). Notice also that the only way to have zero density and zero
 427 internal energy on a set of nonzero measure is when vacuum is present in the solution and $v_L^* < v_R^*$;
 428 in this case, $\lambda_L^- < \lambda_L^+$ and $\lambda_R^- < \lambda_R^+$ and the density and the internal energy are positive in the
 429 regions $\frac{x}{t} \in [\lambda_L^-, \lambda_L^+)$, $\frac{x}{t} \in (\lambda_R^-, \lambda_R^+]$. Consider the concave functionals $\tilde{\Psi}_1 : \tilde{\mathbf{u}} \mapsto \rho$, $\tilde{\Psi}_2 : \tilde{\mathbf{u}} \mapsto 1 - b\rho$,
 430 and $\tilde{\Psi}_3 : \tilde{\mathbf{u}} \mapsto \rho e$. Notice that $\tilde{\Psi}_l(\tilde{\mathbf{U}}_j^n) > 0$ for all $j \in \mathcal{G}(i)$ and all $l \in \{1:3\}$ whether vacuum
 431 occurs or not. We conclude that $\tilde{\Psi}_l(\tilde{\mathbf{U}}_{ij}^n) > 0$ for all $l \in \{1:3\}$ by invoking Item (iv) in Lemma 3.2.
 432 But the identity (3.5) shows that the density and the internal energy of the states $\overline{\mathbf{U}}_{ij}^n$ and $\tilde{\mathbf{U}}_{ij}^n$
 433 are identical; as a result, defining $\Psi_1 : \mathbf{u} \mapsto \rho$, $\Psi_2 : \mathbf{u} \mapsto 1 - b\rho$, and $\Psi_3 : \mathbf{u} \mapsto \rho e$, we infer that
 434 $\Psi_l(\overline{\mathbf{U}}_{ij}^n) = \tilde{\Psi}_l(\tilde{\mathbf{U}}_{ij}^n) > 0$ for all $l \in \{1:3\}$. This establishes that $\overline{\mathbf{U}}_{ij}^n \in \mathcal{B}(b)$.

435 (ii) The assertion follows from (i), the convexity of $\mathcal{B}(b)$, and the observation that (2.9) implies that
 436 \mathbf{U}_i^{n+1} is in the convex hull of $\{\overline{\mathbf{U}}_{ij}^n \mid j \in \mathcal{G}(i)\}$ if $\tau \sum_{j \in \mathcal{G}(i) \setminus \{i\}} \frac{2d_{ij}^n}{m_i} \leq 1$. This completes the proof. \square

437 Theorem 4.6 says that the algorithm (2.7) is invariant-domain preserving under the appropriate
 438 CFL condition. To make this theorem useful, we now need to derive a computable upper bound on
 439 the maximum wave speed in the extended Riemann problem (3.4). This task is achieved in §5.

440 **5. Upper bound on the maximum wave speed.** Setting $\lambda_{\max}(p) := \max(-\lambda_L^-(p), \lambda_R^+(p))$,
 441 we recall that the maximum wave speed in the Riemann problem (3.4) is given by $\lambda_{\max}(p^*)$. Recall
 442 also that $p \mapsto \lambda_{\max}(p)$ is a nondecreasing function. Since we only need an upper bound on $\lambda_{\max}(p^*)$,
 443 we derive in this section an explicit upper bound on p^* .

444 **5.1. Motivation and notation.** We recall that $p^* = 0$ if vacuum is present, and the max-
 445 imum speed of propagation is then $\lambda_{\max}(0) = \max(|v_L - a_L|, |v_R + a_R|)$. (The L-wave and the
 446 R-wave are both expansions in this case.) If the non-vacuum condition holds (see (4.3)), p^* solves

447 the equation

$$448 \quad \phi(p) = f_L(p) + f_R(p) + v_R - v_L = 0, \quad p \in (0, \infty).$$

449 As proved in Guermond and Popov [11, Lem. 4.2], a simple upper bound for p^* can be obtained by
 450 using the so called double-rarefaction approximation (see also Pike [23]), which consists of finding
 451 the unique root of the modified equation $\phi_{RR}(p) = 0$, where

$$452 \quad (5.1) \quad \phi_{RR}(p) := \frac{2a_L(1-b\rho_L)}{\gamma_L-1} \left(\left(\frac{p}{p_L} \right)^{\frac{\gamma_L-1}{2\gamma_L}} - 1 \right) + \frac{2a_L(1-b\rho_R)}{\gamma_R-1} \left(\left(\frac{p}{p_R} \right)^{\frac{\gamma_R-1}{2\gamma_R}} - 1 \right) + v_R - v_L.$$

453 It can be shown that $\phi_{RR}(p) \leq \phi(p)$ for all $p \in [\min(p_L, p_R), \infty)$ if $\max(\gamma_L, \gamma_R) \in (1, \frac{5}{3}]$. Using
 454 the notation from (4.1), this result is proved in [11, Lem. 4.2] by showing that $f_Z^S(p) \geq f_Z^R(p)$
 455 for all $p > p_Z$ if $\gamma_Z \in (1, \frac{5}{3}]$. We revisit this idea in the rest of §5 and remove the assumption
 456 $\max(\gamma_L, \gamma_R) \in (1, \frac{5}{3}]$. More precisely, we use a result from Theorem A.2 proved in Appendix A:
 457 there exists a function $c(\gamma_Z)$ (defined in (A.3)) so that $f_Z^S(p) \geq c(\gamma_Z)f_Z^R(p)$ for all $p > p_Z$. This
 458 function is equal to 1 over the range $\gamma_Z \in (1, \frac{5}{3}]$ and decreases monotonically to $\frac{1}{\sqrt{2}}$ as γ_Z grows to
 459 infinity. To simplify the notation, let us set $\alpha_Z := c(\gamma_Z) \frac{2a_Z(1-b\rho_Z)}{\gamma_Z-1}$. We then redefine ϕ_{RR} for all
 460 $\gamma_Z \in (1, \infty)$ by setting

$$461 \quad (5.2) \quad \phi_{RR}(p) := \alpha_L \left(\left(\frac{p}{p_L} \right)^{\frac{\gamma_L-1}{2\gamma_L}} - 1 \right) + \alpha_R \left(\left(\frac{p}{p_R} \right)^{\frac{\gamma_R-1}{2\gamma_R}} - 1 \right) + v_R - v_L.$$

462 We then have $\phi_{RR}(p) \leq \phi(p)$ for all $p \in [\min(p_L, p_R), \infty)$ and all $\gamma_Z \in (1, \infty)$.

463 When $\gamma_L = \gamma_R$ (i.e., the case of the ideal gas law) the equation $\phi_{RR}(p) = 0$ can be easily solved
 464 since it is linear up to a trivial change of variable. But solving $\phi_{RR}(p) = 0$ in the general case (i.e.,
 465 $\gamma_L \neq \gamma_R$) is far more difficult since the equation is nonlinear. In the rest of §5 we extract further
 466 lower bounds on ϕ_{RR} to derive an explicit upper bound on p^* .

467 To simplify the notation in many of the expressions used below, we introduce two indices in
 468 the set $\{L, R\}$ denoted by “min” and “max” and defined as follows:

$$469 \quad (5.3) \quad \min := \begin{cases} L & \text{if } p_L \leq p_R, \\ R & \text{if } p_L > p_R, \end{cases} \quad \max := \begin{cases} R & \text{if } p_L \leq p_R, \\ L & \text{if } p_L > p_R. \end{cases}$$

470 Notice that $p_{\min} = \min(p_L, p_R)$, $p_{\max} = \max(p_L, p_R)$. For instance $a_{\min} = a_Z$ and $\gamma_{\min} = \gamma_Z$
 471 if $p_{\min} = p_Z$, and $a_{\max} = a_Z$ and $\gamma_{\max} = \gamma_Z$ if $p_{\max} = p_Z$. We also introduce the two indices
 472 $m \in \{L, R\}$ and $M \in \{L, R\}$ defined as follows:

$$473 \quad (5.4) \quad m := \begin{cases} L & \text{if } \gamma_L \leq \gamma_R, \\ R & \text{if } \gamma_L > \gamma_R, \end{cases} \quad M := \begin{cases} R & \text{if } \gamma_L \leq \gamma_R, \\ L & \text{if } \gamma_L > \gamma_R. \end{cases}$$

474 Notice that $\gamma_m = \min(\gamma_L, \gamma_R)$ and $\gamma_M := \max(\gamma_L, \gamma_R)$. However, γ_{\min} and γ_{\max} may not coincide
 475 with the values γ_m and γ_M , respectively. We now propose an upper bound on p^* based on the signs
 476 of $\phi(p_{\min})$ and $\phi(p_{\max})$.

477 **5.2. Case 0: vacuum.** If the vacuum condition holds, i.e., $v_R - v_L \geq \frac{2a_L(1-b\rho_L)}{\gamma_L-1} + \frac{2a_R(1-b\rho_R)}{\gamma_R-1}$,
 478 we have $p^* = 0$ and $\lambda_{\max}(0) = \max(|v_L - a_L|, |v_R + a_R|)$.

479 **5.3. Case 1:** $0 < p^*$ and $0 < \phi(p_{\min})$. This case corresponds to the L-wave and the R-wave
 480 both being expansion waves. In this case $p^* < p_{\min}$, which means that we do not need to compute
 481 p^* as we have $\lambda_1^-(p^*) = v_L - a_L$ and $\lambda_3^+(p^*) = v_R + a_R$. But, if for some reason an upper bound
 482 for p^* is needed, one can use the root of the function

$$483 \quad (5.5) \quad \widehat{\phi}_{RR}(p) := \alpha_R \left(\left(\frac{p}{p_R} \right)^{\frac{\gamma_M-1}{2\gamma_M}} - 1 \right) + \alpha_L \left(\left(\frac{p}{p_L} \right)^{\frac{\gamma_M-1}{2\gamma_M}} - 1 \right) + v_R - v_L.$$

484 Note that $\widehat{\phi}_{RR}(p) \leq \phi_{RR}(p) = \phi(p)$ for all $p \in [0, p_{\min}]$. We give the root for completeness,

$$485 \quad (5.6) \quad \widehat{p}^* = \left(\frac{\alpha_R + \alpha_L - (v_R - v_L)}{\alpha_R p_R^{-\frac{\gamma_M-1}{2\gamma_M}} + \alpha_L p_L^{-\frac{\gamma_M-1}{2\gamma_M}}} \right)^{\frac{2\gamma_M}{\gamma_M-1}}.$$

486 We have that $p^* = \widehat{p}^* \leq \widehat{p}^*$. In conclusion, an upper bound on p^* is $\min(p_{\min}, \widehat{p}^*)$. This im-
 487 plies that $0 < p^* \leq \min(p_{\min}, \widehat{p}^*)$. Notice in passing that $\lambda_1^-(\min(p_{\min}, \widehat{p}^*)) = v_L - a_L$ and
 488 $\lambda_3^+(\min(p_{\min}, \widehat{p}^*)) = v_R + a_R$.

489 **5.4. Case 2:** $\phi(p_{\min}) < 0 < \phi(p_{\max})$. In this case the min-wave is a shock and the max-wave
 490 is an expansion. Here we have $p_{\min} < p^* < p_{\max}$ and so for $p \in (p_{\min}, p_{\max})$ we have that

$$491 \quad (5.7) \quad \phi_{RR}(p) = \alpha_{\min} \left(\left(\frac{p}{p_{\min}} \right)^{\frac{\gamma_{\min}-1}{2\gamma_{\min}}} - 1 \right) + \alpha_{\max} \left(\left(\frac{p}{p_{\max}} \right)^{\frac{\gamma_{\max}-1}{2\gamma_{\max}}} - 1 \right) + v_R - v_L.$$

492 We consider two cases to derive a lower bound on $\phi_{RR}(p)$. If $\gamma_{\min} = \gamma_m$, we define

$$493 \quad \widehat{\phi}_1(p) := \alpha_{\min} \left(\left(\frac{p}{p_{\min}} \right)^{\frac{\gamma_M-1}{2\gamma_M}} r - 1 \right) + \alpha_{\max} \left(\left(\frac{p}{p_{\max}} \right)^{\frac{\gamma_M-1}{2\gamma_M}} - 1 \right) + v_R - v_L,$$

$$494 \quad \widehat{\phi}_2(p) := \alpha_{\min} \left(\left(\frac{p}{p_{\min}} \right)^{\frac{\gamma_m-1}{2\gamma_m}} - 1 \right) + \alpha_{\max} \left(\left(\frac{p}{p_{\max}} \right)^{\frac{\gamma_m-1}{2\gamma_m}} r - 1 \right) + v_R - v_L,$$

496 where $r := \left(\frac{p_{\min}}{p_{\max}} \right)^{\frac{\gamma_M-\gamma_m}{2\gamma_m\gamma_M}}$. We have $\max(\widehat{\phi}_1(p), \widehat{\phi}_2(p)) \leq \phi_{RR}(p)$ for all $p \in (p_{\min}, p_{\max})$. Solving
 497 $\widehat{\phi}_1(p) = 0$ and $\widehat{\phi}_2(p) = 0$ gives

$$498 \quad \widehat{p}_1^* = \left(\frac{\alpha_{\min} + \alpha_{\max} - (v_R - v_L)}{r\alpha_{\min}p_{\min}^{-\frac{\gamma_M-1}{2\gamma_M}} + \alpha_{\max}p_{\max}^{-\frac{\gamma_M-1}{2\gamma_M}}} \right)^{\frac{2\gamma_M}{\gamma_M-1}}, \quad \widehat{p}_2^* = \left(\frac{\alpha_{\min} + \alpha_{\max} - (v_R - v_L)}{\alpha_{\min}p_{\min}^{-\frac{\gamma_m-1}{2\gamma_m}} + r\alpha_{\max}p_{\max}^{-\frac{\gamma_m-1}{2\gamma_m}}} \right)^{\frac{2\gamma_m}{\gamma_m-1}}.$$

500 Hence, an upper bound on p^* is $\min(p_{\max}, \widehat{p}_1^*, \widehat{p}_2^*)$ if $\gamma_{\min} = \gamma_m$. This implies that $p_{\min} < p^* \leq$
 501 $\min(p_{\max}, \widehat{p}_1^*, \widehat{p}_2^*)$. In the other case, $\gamma_{\min} = \gamma_M$, we have $\gamma_{\max} = \gamma_m$ and two lower bounds on $\widehat{\phi}(p)$
 502 are given by

$$503 \quad \widehat{\phi}_1(p) := \alpha_{\min} \left(\left(\frac{p}{p_{\min}} \right)^{\frac{\gamma_m-1}{2\gamma_m}} - 1 \right) + \alpha_{\max} \left(\left(\frac{p}{p_{\max}} \right)^{\frac{\gamma_m-1}{2\gamma_m}} - 1 \right) + v_R - v_L,$$

$$504 \quad \widehat{\phi}_2(p) := \alpha_{\min} \left(\left(\frac{p}{p_{\min}} \right)^{\frac{\gamma_M-1}{2\gamma_M}} - 1 \right) + \alpha_{\max} \left(\left(\frac{p}{p_{\max}} \right)^{\frac{\gamma_M-1}{2\gamma_M}} - 1 \right) + v_R - v_L.$$

505

506 Again, the equations $\widehat{\phi}_1(p) = 0$, $\widehat{\phi}_2(p) = 0$ are linear (up to a change of variable). The roots are

$$507 \quad \widehat{p}_1^* = \left(\frac{\alpha_{\min} + \alpha_{\max} - (v_R - v_L)}{\alpha_{\min} p_{\min}^{-\frac{\gamma_m-1}{2\gamma_m}} + \alpha_{\max} p_{\max}^{-\frac{\gamma_m-1}{2\gamma_m}}} \right)^{\frac{2\gamma_m}{\gamma_m-1}}, \quad \widehat{p}_2^* = \left(\frac{\alpha_{\min} + \alpha_{\max} - (v_R - v_L)}{\alpha_{\min} p_{\min}^{-\frac{\gamma_M-1}{2\gamma_M}} + \alpha_{\max} p_{\max}^{-\frac{\gamma_M-1}{2\gamma_M}}} \right)^{\frac{2\gamma_M}{\gamma_M-1}}.$$

509 An upper bound on p^* is $\min(p_{\max}, \widehat{p}_1^*, \widehat{p}_2^*)$ if $\gamma_{\min} = \gamma_M$. Hence $p_{\min} < p^* \leq \min(p_{\max}, \widehat{p}_1^*, \widehat{p}_2^*)$.

510 **5.5. Case 3:** $\phi(p_{\max}) < 0$. In this case we have $p_{\max} < p^*$ and the L-wave and the R-wave
511 are shocks. We bound $\phi_{RR}(p)$ from below by the function,

$$512 \quad (5.8) \quad \widehat{\phi}(p) := \alpha_L \left(\left(\frac{p}{p_L} \right)^{\frac{\gamma_m-1}{2\gamma_m}} - 1 \right) + \alpha_R \left(\left(\frac{p}{p_R} \right)^{\frac{\gamma_m-1}{2\gamma_m}} - 1 \right) + v_R - v_L.$$

513 The corresponding root for $\widehat{\phi}(p) = 0$ is

$$514 \quad (5.9) \quad \widehat{p}_1^* = \left(\frac{\alpha_L + \alpha_R - (v_R - v_L)}{\alpha_L p_L^{-\frac{\gamma_m-1}{2\gamma_m}} + \alpha_R p_R^{-\frac{\gamma_m-1}{2\gamma_m}}} \right)^{\frac{2\gamma_m}{\gamma_m-1}}.$$

515 Another possibility consists of observing that ϕ is the sum of two shock curves plus the constant
516 $v_R - v_L$. Observing that $B_Z \leq B_Z p p_{\max}^{-1}$ for all $p \in (p_{\max}, \infty)$, we infer that the graph of the
517 following function is also below the graph of ϕ :

$$518 \quad (5.10) \quad \widehat{\phi}(p) := \frac{p - p_L}{\sqrt{p}} \left(\frac{A_L}{1 + \frac{B_L}{p_{\max}}} \right)^{\frac{1}{2}} + \frac{p - p_R}{\sqrt{p}} \left(\frac{A_R}{1 + \frac{B_R}{p_{\max}}} \right)^{\frac{1}{2}} + v_R - v_L.$$

519 Let $x_Z := \left(\frac{A_Z}{1 + B_Z p_{\max}^{-1}} \right)^{\frac{1}{2}}$, $a := x_L + x_R$, $b := v_R - v_L$, $c := -p_L x_L - p_R x_R$, then the only positive
520 root of $\widehat{\phi}$ is

$$521 \quad (5.11) \quad \widehat{p}_2^* = \left(\frac{-b + (b^2 - 4ac)^{\frac{1}{2}}}{2a} \right)^2.$$

522 An upper bound on p^* is $\min(\widehat{p}_1^*, \widehat{p}_2^*)$. Hence $p_{\max} < p^* \leq \min(\widehat{p}_1^*, \widehat{p}_2^*)$.

523 **5.6. Iterative solution.** Another possibility to estimate p^* from above consists of solving
524 $\phi(p) = 0$ by using the iterative quadratic Newton method described in Guermond and Popov [11,
525 Alg. 1]. The method is guaranteed to be convergent since the function ϕ defined in (4.2) is concave.
526 Using the lower and upper bounds provided in §5.3–§5.5, the method is also guaranteed to deliver
527 an upper bound on p^* for every termination threshold since $\phi'''(\xi) > 0$ for all $\xi > 0$ (see the proof
528 of Lemma 4.5 in [11]). A source code for this method is publicly available at [3].

529 **6. Numerical Results.** We numerically illustrate in this section the algorithm (2.7) with the
530 viscosity defined in Theorem 4.6 using the explicit upper bound \widehat{p}^* defined in §5.2–5.5.

531 **6.1. Convergence tests.** We use the van der Waals equation of state as the oracle to validate
532 the method. More precisely, we consider the solution to a Riemann problem and compare it to the
533 numerical approximation (2.7) where the viscosity d_{ij}^n is defined in (4.14b) with \widehat{p}^* being the upper

534 bound on p^* derived in §5.2–§5.5. Recall that for the van der Waals equation of state, the pressure
 535 is given by $p(\rho, e) := (\gamma - 1) \frac{\rho e + a \rho^2}{1 - b \rho} - a \rho^2$, where γ , a and b are constants depending on the nature
 536 of the fluid (see e.g., Callen [2, §3.5], Fossati and Quartapelle [9, §6.3]). We select the parameters γ ,
 537 a , b so that the problem is hyperbolic and the solution exhibits a composite wave structure: we use
 538 $\gamma = 1.02$, $a = 1$, $b = 1$. With these parameters the isentropes in the $(p, \frac{1}{\rho})$ diagram are nonconvex.
 539 The loss of convexity is necessary for the existence of composite waves. The initial left and right
 540 states we choose are:

$$541 \quad (6.1) \quad \begin{aligned} (\rho_L, v_L, p_L) &:= (0.10, -0.475504638574729, 0.022084258693080), \\ (\rho_R, v_R, p_R) &:= (0.39, -0.121375781741349, 0.039073167077590). \end{aligned}$$

542 The exact solution is a 3-wave composed of an expansion fan, a shock, and another expansion fan.
 543 The details of the construction of the solution can be found in Cramer and Sen [6], Lai [17], and
 544 Fossati and Quartapelle [9, §6.4]. For completeness and reproducibility, the construction of the
 545 exact solution is given in the supplementary material and a code computing the exact solution is
 546 available at Clayton et al. [4].

#dof	$\delta_1(t)$	rate	$\delta_2(t)$	rate
101	2.14E-01	–	2.67E-01	–
201	1.44E-01	0.58	2.07E-01	0.37
401	9.40E-02	0.62	1.58E-01	0.39
801	5.96E-02	0.66	1.20E-01	0.40
1601	3.66E-02	0.70	8.96E-02	0.42
3201	2.18E-02	0.75	6.66E-02	0.43
6401	1.27E-02	0.78	4.93E-02	0.43
12801	7.26E-03	0.81	3.66E-02	0.43
25601	4.09E-03	0.83	2.72E-02	0.43

Table 1: Consolidated errors and convergence rates. Solution computed at $t = 5.0$.

547 We approximate the solution with \mathbb{P}_1 continuous finite elements in one dimension. The com-
 548 putational domain is $D := (-1, 1)$ with CFL=0.5. The estimation of the maximum wave speed
 549 (see (4.14a)) is done by using \hat{p}^* as explained in §5.2–§5.5. A series of computations is done on nested
 550 uniform meshes to estimate the convergence rate of the method. Denoting by $(\rho_h(t), \mathbf{m}_h(t), E_h(t))$
 551 the approximation at time t , we compute a consolidated error indicator by adding the relative error
 552 in the L^q -norm on the density, the momentum, and the total energy as follows:

$$553 \quad (6.2) \quad \delta_q(t) := \frac{\|\rho_h(t) - \rho(t)\|_{L^q(D)}}{\|\rho(t)\|_{L^q(D)}} + \frac{\|\mathbf{m}_h(t) - \mathbf{m}(t)\|_{L^q(D)}}{\|\mathbf{m}(t)\|_{L^q(D)}} + \frac{\|E_h(t) - E(t)\|_{L^q(D)}}{\|E(t)\|_{L^q(D)}}.$$

555 The results of the convergence tests are reported in Table 1. The number of grid points is reported
 556 in the leftmost column. The errors are computed at $t = 0.5$. We observe that the method is
 557 convergent, and the convergence rates are consistent with the approximation being formally first-
 558 order accurate.

559 **6.2. The two-expansion-wave-speed estimate.** It is often reported in the literature that,
 560 for practical purpose, one can use the two expansion wave speeds, $v_L - c_L$, $v_R + c_R$, to estimate

561 the maximum wave speed. Using the covolume equation of state, we have shown in [11, App. B]
 562 that $\max(|v_L - c_L|, |v_R + c_R|)$ is not an upper bound on the maximum wave speed in the Riemann
 563 problem. But the reader could legitimately be skeptical about this kind of theoretical result and
 564 may wonder whether these academic arguments have any impact on practical computations. We
 565 now illustrate that the two-expansion-wave-speed estimate is not robust: it can either lead to an
 566 underestimation or to an overestimation of the viscosity with severe consequences in both cases.

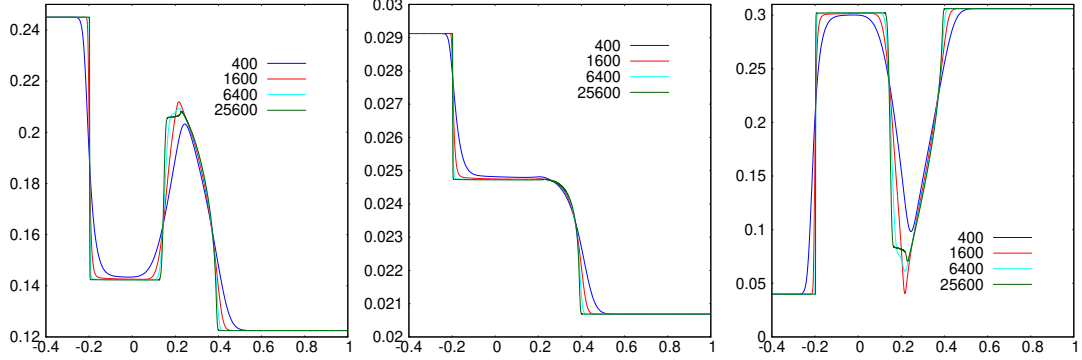


Fig. 1: Test with the data (6.3), $t = 1.25$. From left to right: density, pressure, sound speed.

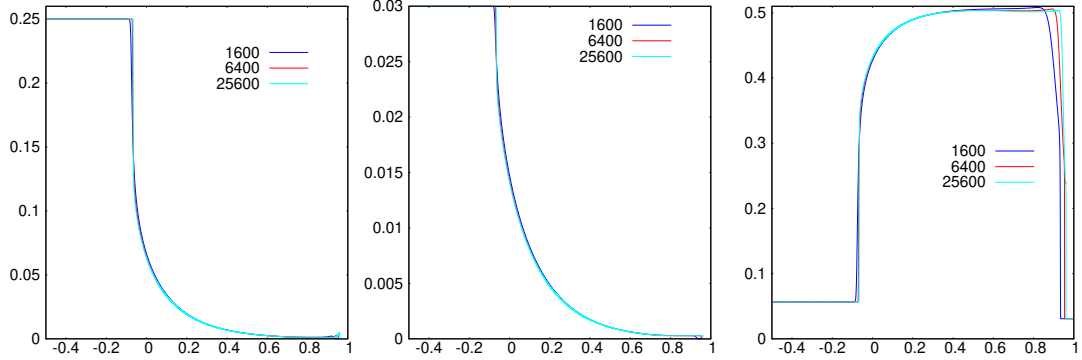


Fig. 2: Test with the data (6.4), $t = 0.4$. From left to right: density, pressure, sound speed.

567 We start by showing that $\max(|v_L - c_L|, |v_R + c_R|)$ can lead to an underestimation of the
 568 viscosity and therefore lead to violations of important properties. Our oracle is the van der Waals
 569 equation of state with $a = 1$, $b = 1$, $\gamma = 1.02$. We solve two Riemann problems. The first one is
 570 equipped with the following data set:

$$571 \quad (6.3) \quad \begin{aligned} (\rho_L, v_L, p_L) &:= (0.2450, 0, 2.9123894332846005 \times 10^{-2}), \\ (\rho_R, v_R, p_R) &:= (0.1225, 0, 2.0685894810791836 \times 10^{-2}), \end{aligned}$$

572 which gives the sound speeds $(c_L, c_R) \approx (0.00399, 0.306)$. The second one is equipped with the

573 following data set:

$$574 \quad (6.4) \quad \begin{aligned} (\rho_L, v_L, p_L) &:= (2.5 \times 10^{-1}, 0, 3 \times 10^{-2}), \\ (\rho_R, v_R, p_R) &:= (4.9 \times 10^{-5}, 0, 5 \times 10^{-8}), \end{aligned}$$

575 which gives the sound speeds $(c_L, c_R) \approx (0.057, 0.031)$. For each data set, we perform two series of
 576 computations on the domain $D = (-0.5, 1)$. The computations are done up to $t = 1.25$ for the first
 577 data set and up to $t = 0.4$ for the second data set. In both cases we use $\text{CFL} = 0.5$. One series
 578 of computations is done with the estimation of the maximum wave speed (see (4.14a)) using \hat{p}^* as
 579 explained in §5.2–§5.5 (no iteration is done). The other one is done using the two-expansion-wave-
 580 speed estimate $\max(|v_L - c_L(p_L, \rho_L)|, |v_R + c_R(p_L, \rho_L)|)$ with $c(p, \rho) = (\gamma \frac{p+a\rho^2}{\rho(1-b\rho)} - 2a\rho)^{\frac{1}{2}}$. It turns
 581 out that the computations done with the two-expansion-wave-speed estimate violates the invariant
 582 domain property after a few time steps for both data sets: one obtains a complex sound speed
 583 for the first data set and one obtains a negative internal energy for the second data set. These
 584 violations occur no matter how small the CFL number is. The computations done with the method
 585 proposed in the paper run without any problem. We show in Figure 1 the density, the pressure and
 586 the sound speed profiles for various mesh sizes $(\frac{1.5}{100}, \frac{1.5}{400}, \frac{1.5}{1600}, \frac{1.5}{25600})$ for the data set (6.3). The
 587 results for the second data set (6.4) are shown in Figure 2 with the mesh sizes $\frac{1.5}{1600}, \frac{1.5}{6400}$. Notice
 588 that in both cases the R-wave is a composite wave composed of an expansion followed by a shock.

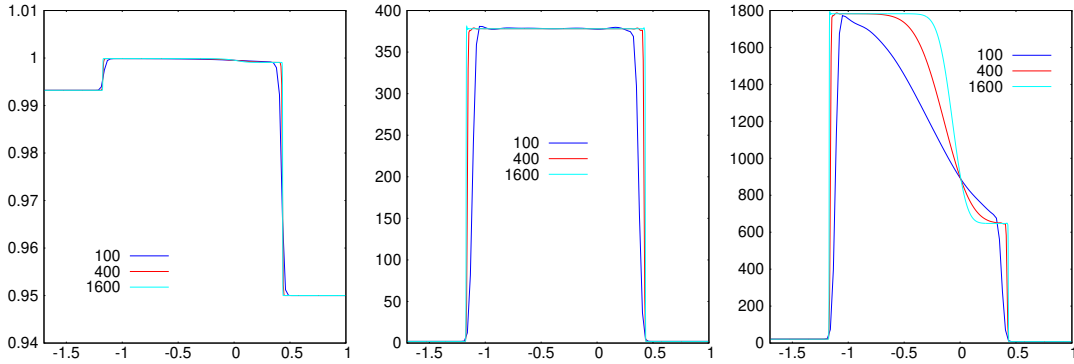


Fig. 3: Test with the data (6.5), $t = 0.005$. From left to right: density, pressure, sound speed.

589 We now show that the two-expansion-wave-speed estimate can lead to a local overestimation
 590 of the viscosity and thereby to a reduction of the admissible range of time step sizes. We use again
 591 the van der Waals equation of state with the same parameters as above for the oracle. We consider
 592 the Riemann problem with the following data:

$$593 \quad (6.5) \quad \begin{aligned} (\rho_L, v_L, p_L) &:= (0.9932, 3, 2), \\ (\rho_R, v_R, p_R) &:= (0.9500, -3, 2). \end{aligned}$$

594 The corresponding sound speeds are $(c_L, c_R) \approx (21.2, 7.77)$. The computational domain is $D =$
 595 $(-1.7, 1)$ and the computations are done up to $t = 0.005$. For the computation with the two-
 596 expansion-wave-speed, the CFL number needed to avoid producing negative internal energy is
 597 about 0.06. The maximal admissible CFL number for the present method is about 0.71 (i.e., below

598 this CFL number the sound speed is real and the internal energy is positive at every grid point and
 599 for every time step). As a result the computational cost of the method using the two-expansion-
 600 wave-speed estimate is almost 12 times higher than that of the present method. We show in Figure 3
 601 the density, the pressure and the sound speed for various meshes using the present method. The
 602 results obtained with the two-expansion-wave-speed estimate are almost identical (not shown).

603 **6.3. Further illustrations.** We continue by illustrating the proposed method by using a
 604 cubic equation of state as the oracle, see Redlich and Kwong [25], Valderrama [29]. We refer the
 605 reader to Dumbser and Casulli [8] where series of tests are done with this type of equation of state.
 606 For a general cubic equation of state, the pressure is given by

$$607 \quad (6.6) \quad p(\rho, e) = \frac{R\rho T(\rho, e)}{1 - b\rho} - \frac{\alpha\rho^2}{\sqrt{T(\rho, e)}(1 - br_1\rho)(1 - br_2\rho)},$$

608 where $T(\rho, e)$ solves the following cubic equation:

$$609 \quad (6.7) \quad e = c_v T + \frac{3\alpha}{2b\sqrt{T}} \frac{1}{r_1 - r_2} \log\left(\frac{1 - br_1\rho}{1 - br_2\rho}\right).$$

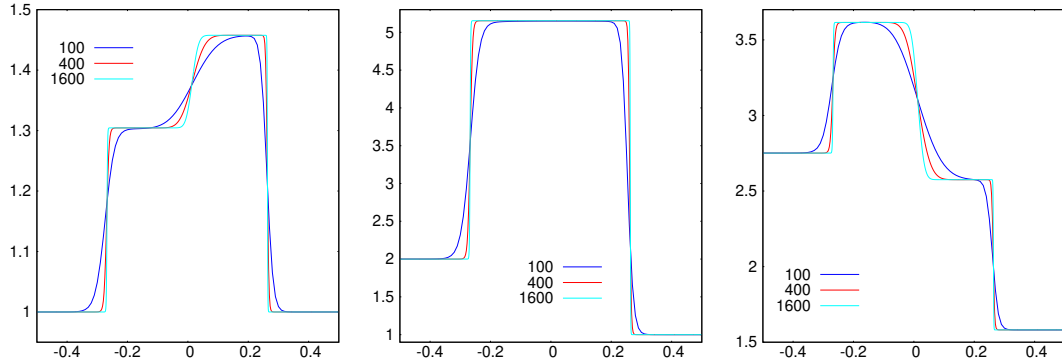


Fig. 4: Test with the data (6.8), $t = 0.1$. From left to right: density, pressure, temperature.

610 We take $r_1 = 0$ and $r_2 = -1$ (this corresponds to the so-called Redlich-Kwong equation). We
 611 solve two of the problems from [8, §3.3] where $R = 0.4$, $\alpha = 0.5$, $b = 0.5$. These are two Riemann
 612 problems. For the first problem we take $c_v = 1$ and the initial data are

$$613 \quad (6.8) \quad \begin{aligned} (\rho_L, v_L, p_L) &:= (1, 1, 2), \\ (\rho_R, v_R, p_R) &:= (1, -1, 1). \end{aligned}$$

614 The computational domain is $(-0.5, 0.5)$ and the final time is $t = 0.1$. For the second problem we
 615 take

$$616 \quad (6.9) \quad \begin{aligned} (\rho_L, v_L, p_L) &:= (1, 0, 1000), \\ (\rho_R, v_R, p_R) &:= (1, 0, 0.01), \end{aligned}$$

617 with $c_v = 1.5$ (we suspect there is a typo in [8, §3.3], since the authors say that they use $c_v = 1$ with
 618 the above data, but this gives a negative internal energy for the right state.) The computational

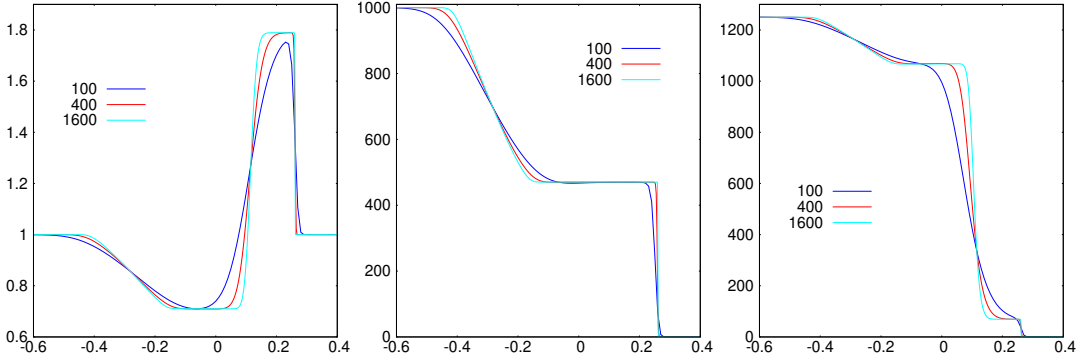


Fig. 5: Test with the data (6.9), $t = 0.008$. From left to right: density, pressure, temperature.

619 domain is $D = (-0.6, 0.4)$ and the final time is $t = 0.008$. In both cases, we take the covolume
 620 constant in (3.2) to be $b = 0.5$ (using $b = 0$ in (3.2) gives similar results, not shown). The CFL
 621 number is 0.5. The results obtained with various meshes are displayed in Figure 4, for the first
 622 case, and in Figure 5, for the second case. In each case, we show the density, the pressure and the
 623 temperature. These results are similar to those reported in [8, §3.3].

624 **6.4. Two-dimensional illustration.** To demonstrate that the proposed method is actually
 625 independent of the space dimension, we illustrate it by using a finite element code which implements
 626 the algorithm (2.7). The documentation of this program is found in Maier and Tomas [21]. We
 627 replace the estimation of $\hat{\lambda}(\mathbf{n}_{ij}, \mathbf{U}_i, \mathbf{U}_j)$ used in this code (and described in [11]) by the estimation
 628 (4.14a) with \hat{p}^* computed as explained in §5.2–§5.5. The oracle is the van der Waals equation of
 629 state with $\gamma = 1.4$, $a = 0.3215$, and $b = 0.1$. The computation of \hat{p}^* is done with the assumption
 630 that $b = 0$. That is, we assume that the covolume constant b is unknown.

631 We simulate the flow around a cylinder in a two-dimensional channel. The computational
 632 domain is $D = (-0.9, 3.1) \times (-1, 1) \setminus C$, with C being the disk of radius 0.15 centered at $(0, 0)$.
 633 We enforce the density, the momentum and the total energy at the inflow boundary, $\{x = -0.9\}$:
 634 $(\rho, \mathbf{m}, E) = (1.4, (4.2, 0)^\top, 9.154375)$. The primitive variable corresponding to these data are $\mathbf{v} =$
 635 $(3, 0)^\top$ and $p = 1$. The corresponding Mach number is 3. The slip boundary condition is enforced at
 636 the top and at the bottom of the channel. Nothing is done at the outflow boundary condition (this
 637 is a supersonic outflow boundary). We use continuous \mathbb{Q}_1 finite elements. We refer the reader to
 638 Maier and Tomas [21] for the implementation details. We show in Figure 6 the density computed
 639 at time $t = 4$ using a Schlieren-like representation. Letting $\sum_{i \in \mathcal{V}} \rho_i^n \varphi_i$ be the approximation of
 640 the density, we approximate the Euclidean norm of the gradient of the density as follows $r_i^n :=$
 641 $m_i^{-1} \|\sum_{j \in \mathcal{G}(D_i)} \mathbf{c}_{ij} \rho_j^n\|_{\ell^2}$, for all $i \in \mathcal{V}$. The values of the Schlieren field are defined at the grid
 642 points by $\exp(-\beta(r_i^n - \min_{j \in \mathcal{G}(i)} r_j^n) / (\max_{j \in \mathcal{G}(i)} r_j^n - \min_{j \in \mathcal{G}(i)} r_j^n))$ where $\beta = 10$. For comparison,
 643 we also show in the right panel of this figure the density obtained at the same time using the ideal
 644 gas equation of state. The inflow boundary data is $(\rho, \mathbf{m}, E) := (1.4, (4.2, 0)^\top, 8.8)$ and $\gamma = 1.4$.
 645 This corresponds to the same primitive state, $\mathbf{v} = (3, 0)^\top$ and $p = 1$, as the simulation with the van
 646 der Waals equation of state. The mesh used for these computations has 1.4×10^6 grid points.

647 Of course, these simulations are first-order accurate in space. Making the approximation higher-
 648 order accurate can be done by implementing the convex limiting technique described in [13, 14].

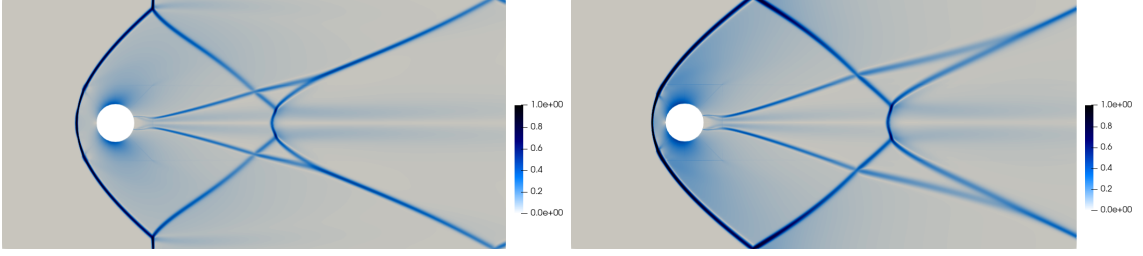


Fig. 6: Cylinder at Mach 3 in a channel. Density, $t = 4$. Left: the oracle is the van der Waals equation of state. Right: the oracle is the ideal gas equation of state with $\gamma = 1.4$.

649 This however requires developing surrogate entropies functionals for the oracle. This task is under
 650 way and the results of this work will be reported elsewhere. We are currently implementing the
 651 technique in the massively parallel code documented in Maier and Kronbichler [20].

652 **7. Conclusions.** We have proposed in the paper an approximation technique for the com-
 653 pressible Euler equations where the equation of state is given by an oracle. The key feature is
 654 an artificial graph viscosity using an estimate on the maximum wave speed on each elementary
 655 Riemann problem that guarantees the positivity of the density and of the internal energy. This
 656 estimate also guarantees an upper bound on the density when a covolume constant is known. The
 657 main theoretical result of the paper is Theorem 4.6. The guaranteed bounds developed in §5.2–
 658 §5.5 are easy to compute. These upper bounds can be used in any algorithm that is based on
 659 approximate Riemann solvers. A computer code implementing all these bounds is freely available
 660 at Clayton et al. [3]. All the simulations reported in the paper have been done with this code.

661 **Acknowledgments.** The authors thank Matthias Maier and Eric Tovar for stimulating dis-
 662 cussions and the help they provided at various stages of this project.

663 **Appendix A. Improvement on the $\gamma > \frac{5}{3}$ estimates.** The objective of this appendix
 664 is to prove that $\phi_{RR}(p) \leq \phi(p)$ for all $p \in [\min(p_L, p_R), \infty)$, where we recall that the function ϕ is
 665 defined in (4.2), the function ϕ_{RR} is defined in (5.1). For future reference we also recall that

$$666 \quad (A.1) \quad f_Z^S(p) := (p - p_Z) \sqrt{\frac{2}{(\gamma_Z + 1)\rho_Z}} \left(p + \frac{\gamma_Z - 1}{\gamma_Z + 1} p_Z \right)^{-\frac{1}{2}} \sqrt{1 - b\rho_Z},$$

$$667 \quad (A.2) \quad f_Z^R(p) := \frac{2\sqrt{\gamma_Z p_Z}}{\gamma_Z - 1} \left(\left(\frac{p}{p_Z} \right)^{\frac{\gamma_Z - 1}{2\gamma_Z}} - 1 \right) \sqrt{1 - b\rho_Z}.$$

668

669 The functions $f_Z^S(p)$ and f_Z^R are, respectively, the shock and rarefaction curves introduced in (4.1).
 670 The following lemma is one of the main result established in Guermond and Popov [11]:

671 **LEMMA A.1** ([11, Lem. 4.2]). *Let $p_Z > 0$, ρ_Z be such that $0 < 1 - b\rho_Z < 1$, and $\gamma_Z \in (1, \infty)$.
 672 Assume that $\gamma \in (1, \frac{5}{3}]$. Then $f_R(p) < f_S(p)$ for all $p \in (p_Z, \infty)$ and $f_R(p_Z) = f_S(p_Z)$, i.e., the
 673 shock curve is above the rarefaction curve.*

674 **THEOREM A.2.** *Assume $\gamma \in (1, \frac{5}{3}]$. Let p_{\min} and p_{\max} be defined as in §5.1. For any $p \geq 0$,*

675 the graph of $\phi(p)$ is above the graph of $\phi_{RR}(p)$; more precisely, $\phi_{RR}(p) = \phi(p)$ for all $p \in [0, p_{\min}]$
 676 and $\phi_{RR}(p) < \phi(p)$ for all $p \in (p_{\min}, \infty)$.

677 *Proof.* Note that the two curves $(p, \phi(p))$ and $(p, \phi_{RR}(p))$ coincide if $p \leq p_{\min}$ because both ϕ
 678 and ϕ_{RR} are the sum of the two rarefaction curves plus the constant $v_R - v_L$. If $p_{\min} < p \leq p_{\max}$
 679 the function $\phi(p)$ is the sum of one rarefaction curve and one shock curve plus the constant $v_R - v_L$.
 680 We then conclude by invoking Lemma A.1 with $(p_Z, \rho_Z) = (p_{\min}, \rho_{\min})$. If $p_{\max} \leq p$ the function
 681 $\phi(p)$ is the sum of two shock curves plus the constant $v_R - v_L$. Now we invoke Lemma A.1 twice
 682 to complete the proof, once with $(p_Z, \rho_Z) = (p_{\min}, \rho_{\min})$ and once with $(p_Z, \rho_Z) = (p_{\max}, \rho_{\max})$. \square

683 The assertion in Lemma A.1 is false when $\frac{5}{3} < \gamma_Z$. To remedy this deficiency, we now define a
 684 new function that is guaranteed to be always under $\phi(p)$ for all $\gamma_Z \in (1, \infty)$ and all $p \in (p_{\min}, \infty)$.
 685 Consider

$$686 \quad (\text{A.3}) \quad c(\gamma_Z) := \begin{cases} 1 & \text{if } 1 < \gamma_Z \leq \frac{5}{3} \\ \left(\frac{1}{2} + \frac{4}{3(\gamma_Z+1)}\right)^{\frac{1}{2}} & \text{if } \frac{5}{3} \leq \gamma_Z \leq 3 \\ \left(\frac{1}{2} + \frac{2}{\gamma_Z-1} 3^{\frac{4-2\gamma_Z}{\gamma_Z-1}}\right)^{\frac{1}{2}} & \text{if } 3 \leq \gamma_Z. \end{cases}$$

687 Notice that $(1, \infty) \ni \gamma_Z \mapsto c(\gamma_Z)$ is continuous and $c(\gamma_Z) \in (\frac{1}{2}, 1]$.

688 LEMMA A.3. Let $p_Z > 0$, ρ_Z be such that $0 < 1 - b\rho_Z < 1$, and $\gamma_Z \in (1, \infty)$. Then
 689 $c(\gamma_Z)f_Z^R(p_Z) = f_Z^S(p_Z) = 0$ and $c(\gamma_Z)f_Z^R(p) < f_Z^S(p)$ for all $p \in (p_Z, \infty)$.

690 *Proof.* The proof of the assertion is in the supplementary material. \square

691 References.

- 692 [1] R. Abgrall and S. Karni. Computations of compressible multifluids. *J. Comput. Phys.*, 169(2):
 693 594–623, 2001.
- 694 [2] H. Callen. *Thermodynamics and an introduction to thermostatistics*, 2nd ed. John Wiley &
 695 Sons, New York, 1985. Second edition.
- 696 [3] B. Clayton, J.-L. Guermond, and B. Popov. Upper bound on the maximum wave speed in
 697 Riemann problems for the Euler equations with tabulated equation of state, apr 2021. URL
 698 <https://doi.org/10.5281/zenodo.4685868>.
- 699 [4] B. Clayton, J.-L. Guermond, and B. Popov. Solution to the double sonic shock Riemann
 700 problem with the van der Waals equation of state, Apr. 2021. URL <https://doi.org/10.5281/zenodo.4685958>.
- 701 [5] P. Colella and H. M. Glaz. Efficient solution algorithms for the Riemann problem for real
 702 gases. *J. Comput. Phys.*, 59(2):264–289, 1985.
- 703 [6] M. S. Cramer and R. Sen. Exact solutions for sonic shocks in van der waals gases. *The Physics*
 704 *of Fluids*, 30(2):377–385, 1987.
- 705 [7] J. K. Dukowicz. A general, noniterative Riemann solver for Godunov’s method. *J. Comput.*
 706 *Phys.*, 61(1):119–137, 1985.
- 707 [8] M. Dumbser and V. Casulli. A conservative, weakly nonlinear semi-implicit finite volume
 708 scheme for the compressible Navier-Stokes equations with general equation of state. *Appl.*
 709 *Math. Comput.*, 272(part 2):479–497, 2016.
- 710 [9] M. Fossati and L. Quartapelle. The riemann problem for hyperbolic equations under a non-
 711 convex flux with two inflection points, 2014. URL <https://arxiv.org/abs/1402.5906>.
- 712 [10] E. Godlewski and P.-A. Raviart. *Numerical approximation of hyperbolic systems of conserva-*
 713 *tion laws*, volume 118 of *Applied Mathematical Sciences*. Springer-Verlag, New York, 1996.

- 715 [11] J.-L. Guermond and B. Popov. Fast estimation from above of the maximum wave speed in the
716 Riemann problem for the Euler equations. *J. Comput. Phys.*, 321:908–926, 2016.
- 717 [12] J.-L. Guermond and B. Popov. Invariant domains and first-order continuous finite element
718 approximation for hyperbolic systems. *SIAM J. Numer. Anal.*, 54(4):2466–2489, 2016.
- 719 [13] J.-L. Guermond, M. Nazarov, B. Popov, and I. Tomas. Second-order invariant domain pre-
720 serving approximation of the Euler equations using convex limiting. *SIAM J. Sci. Comput.*,
721 40(5):A3211–A3239, 2018.
- 722 [14] J.-L. Guermond, B. Popov, and I. Tomas. Invariant domain preserving discretization-
723 independent schemes and convex limiting for hyperbolic systems. *Comput. Methods Appl.*
724 *Mech. Engrg.*, 347:143–175, 2019.
- 725 [15] H. Holden and N. H. Risebro. *Front tracking for hyperbolic conservation laws*, volume 152 of
726 *Applied Mathematical Sciences*. Springer, Heidelberg, second edition, 2015.
- 727 [16] M. J. Ivings, D. M. Causon, and E. F. Toro. On Riemann solvers for compressible liquids.
728 *Internat. J. Numer. Methods Fluids*, 28(3):395–418, 1998.
- 729 [17] G. Lai. Interactions of composite waves of the two-dimensional full Euler equations for van
730 der Waals gases. *SIAM J. Math. Anal.*, 50(4):3535–3597, 2018.
- 731 [18] P. D. Lax. Weak solutions of nonlinear hyperbolic equations and their numerical computation.
732 *Comm. Pure Appl. Math.*, 7:159–193, 1954.
- 733 [19] P. D. Lax. Hyperbolic systems of conservation laws. II. *Comm. Pure Appl. Math.*, 10:537–566,
734 1957.
- 735 [20] M. Maier and M. Kronbichler. Efficient parallel 3d computation of the compressible euler
736 equations with an invariant-domain preserving second-order finite-element scheme, 2021.
- 737 [21] M. Maier and I. Tomas. tamiko/step-69: step-69 v20200305, Mar. 2020. URL [https://doi.org/
738 10.5281/zenodo.3698223](https://doi.org/10.5281/zenodo.3698223).
- 739 [22] C. Pantano, R. Saurel, and T. Schmitt. An oscillation free shock-capturing method for com-
740 pressible van der Waals supercritical fluid flows. *J. Comput. Phys.*, 335:780–811, 2017.
- 741 [23] J. Pike. Riemann solvers for perfect and near-perfect gases. *AIAA Journal*, 31(10):1801–1808,
742 1993.
- 743 [24] L. Quartapelle, L. Castelletti, A. Guardone, and G. Quaranta. Solution of the Riemann
744 problem of classical gasdynamics. *J. Comput. Phys.*, 190(1):118–140, 2003.
- 745 [25] O. Redlich and J. N. S. Kwong. On the thermodynamics of solutions. v. an equation of state.
746 fugacities of gaseous solutions. *Chemical Reviews*, 44(1):233–244, 1949.
- 747 [26] P. L. Roe and J. Pike. Efficient construction and utilisation of approximate riemann solu-
748 tions. In *Proc. of the Sixth Int'l. Symposium on Computing Methods in Applied Sciences and*
749 *Engineering, VI*, pages 499–518, NLD, 1985. North-Holland Publishing Co.
- 750 [27] E. F. Toro. *Riemann solvers and numerical methods for fluid dynamics*. Springer-Verlag,
751 Berlin, third edition, 2009.
- 752 [28] E. F. Toro, C. E. Castro, and B. J. Lee. A novel numerical flux for the 3D Euler equations
753 with general equation of state. *J. Comput. Phys.*, 303:80–94, 2015.
- 754 [29] J. O. Valderrama. The state of the cubic equations of state. *Industrial & Engineering Chemistry*
755 *Research*, 42(8):1603–1618, 2003.